

Colloquium: Hidden Order, Superconductivity and Magnetism – The Unsolved Case of URu₂Si₂

J. A. Mydosh*

Kamerlingh Onnes Laboratory, Leiden University, P.O. Box 9504, NL-2300 RA Leiden, The Netherlands

P. M. Oppeneer†

Department of Physics and Astronomy, Uppsala University, P.O. Box 516, S-75120 Uppsala, Sweden

(Dated: October 23, 2018)

This Colloquium reviews the 25 year quest for understanding the continuous (2nd) order, mean-field-like phase transition occurring at 17.5 K in URu₂Si₂. Since ca. ten years the term hidden order (HO) has been coined and utilized to describe the unknown ordered state, whose origin cannot be disclosed by conventional solid-state probes, such as x-rays, neutrons, or muons. HO is able to support superconductivity at lower temperatures ($T_c \approx 1.5$ K) and when magnetism is developed with increasing pressure both the HO and the superconductivity are destroyed. Other ways of probing the HO are via Rh-doping and very large magnetic fields. During the last few years a variety of advanced techniques have been tested to probe the HO state and their attempts will be summarized. A digest of recent theoretical developments is also included. It is the objective of this survey to shed additional light on the HO state and its associated phases in other materials.

PACS numbers: 71.27.+a, 74.70.Tx; 75.30.Mb

Contents

I. Historical Background	1
II. Introduction to URu ₂ Si ₂	2
III. What is Hidden Order	4
IV. Experimental Survey	5
V. Theoretical Survey	8
VI. High Magnetic Fields and Rh-Doping	11
VII. Present State of HO	12
Acknowledgments	16
References	17
Figures	21

I. HISTORICAL BACKGROUND

Uranium is a most intriguing element, not only in itself but also as a basis for forming a variety of compounds and alloys with unconventional or puzzling physics properties (for recent reviews, see Sechovský and Havela (1998), Santini et al. (1999), Stewart (2006)). Natural or depleted uranium, i.e. containing 99.5 percent ²³⁸U has a

mild alpha radioactivity of 25 kBq/g, which allows U-based samples to be fabricated and studied in university laboratories with a minimum of safety precautions. Following initial discoveries of unexpected superconductivity and heavy-fermion behavior in uranium-based compounds as UBe₁₃ (Ott et al., 1983) and UPt₃ (Stewart et al., 1984) it has become popular to synthesize uranium compounds and to cool these in search for exotic ground states. Over the past 50 or so years many conducting and insulating systems were synthesized, analyzed and structurally characterized (Sechovský and Havela, 1998; Stewart, 2001, 2006). The usual classification of the metallic samples at low temperature is superconducting and/or magnetic or with some of the modern compounds designated as “exotic” (Pfleiderer, 2009).

Why are uranium-based materials so interesting? The observed variety of unusual behaviors derive directly from the U open 5*f* shell. Several defining electronic structure quantities of the U *f* electrons are all on the same energy scale: the exchange interaction, 5*f* bandwidth, the spin-orbit interaction, and intra-atomic *f* – *f* Coulomb interaction. As a consequence, i) elemental uranium displays intermediate behavior between the transition metals and the rare-earths in their characteristic bandwidths, yet it generates the largest spin-orbit coupling. ii) U lies directly on the border between localized and itinerant (or overlapping) 5*f* wavefunctions. iii) The Wigner-Seitz radii R_{WS} of comparative elements places U near the minimum between metallic and atomic 5*f* wave functions. And iv) Ionic U can adopt six different valences when combined with other elements, usually one finds U⁴⁺ with two 5*f* electrons or U³⁺ with three 5*f* electrons. However, it is difficult to distinguish or separate

*Electronic address: mydosh@physics.leidenuniv.nl

†Electronic address: peter.oppeener@physics.uu.se

these two valences in metallic systems with strongly hybridized f states which will then play a major role in the ground state properties. So we now have available a weakly radioactive element that can be tuned into unique chemical and electronic states thereby producing its exotic low temperature behavior. Unfortunately moving to the right along the actinide series involves strong radioactive emissions making low temperature physical studies prohibitive except at specially equipped central facilities. The R_{WS} of elemental uranium overlaps with that of hafnium and is yet far away from the nearly constant R_{WS} of the rare earths. Yet Hf is more a superconducting basis than a magnetic one while U sits on the “fence” between superconductivity and magnetism (Smith and Kmetko, 1983)). For a historical review of the actinides, see Moore and van der Laan (2009).

As a traditional way of comparing the various U-based compounds the now-famous Hill plot (Hill, 1970) is most useful. Here one plots the ordering temperature (magnetic and/or superconducting) against the nearest neighbor U–U spacings. According to the trends shown in Fig. 1 for small U–U distances superconducting compounds should be prominent. In the opposite limit at large spacings greater than 3.5 Å, significant magnetic transitions are found. The position of URu₂Si₂ has been added in Fig. 1 where the superconducting and hidden-order transitions span the superconducting/magnetic line. Many of the “exotic” or strongly correlated intermetallic compounds, e.g., UBe₁₃ and UPt₃ do not obey Hill’s rule due to their strong hybridization of the 5*f* electrons with the conduction electrons regardless of the U–U overlap.

Among the exotic U-based compounds there are nine unconventional superconductors which are combined with magnetism (ferromagnetism and antiferromagnetism) or nearly magnetic (spin fluctuations, tiny moments or enhanced susceptibility) behaviors. For such systems the appellation “heavy fermion” has been applied along with “non-Fermi liquid” to describe their deviant behavior. Table III in Pfeleiderer (2009) surveys these materials among which UBe₁₃, UPt₃, and URu₂Si₂ are the most perplexing. From this table we can discern that magnetism plays a major role in the superconductivity, sometimes generating it, sometimes destroying it as we will see below. Here we have a comparison of these different materials which have been the subject of considerable research since the early 1980’s (Pfeleiderer, 2009).

II. INTRODUCTION TO URu₂Si₂

Only for one system, *viz.* URu₂Si₂, has there been continuing and intense interest for the past 25 years. In 1984 a poster by Schlabitz et al. (unpublished) was presented at a fluctuating valence conference in Cologne showing the appearance of two transitions: one superconducting, the other antiferromagnetic. There was no publication of these results (Schlabitz et al., 1986) until after two letter publications appeared in 1985 (Palstra et al., 1985)

and 1986 (Maple et al., 1986). While all three groups agreed on the bulk superconductivity at ≈ 1.0 K, there were different interpretations for the magnetic transition at 17.5 K. Palstra et al. (1985) designated it a weak type of itinerant antiferromagnetism, Maple et al. (1986) a static charge density wave (CDW) or spin-density wave (SDW) transition, and Schlabitz et al. (1986) a local U-moment antiferromagnet. We now know after 25 years that all three interpretations were incorrect. The transition at 17.5 K is not due to long-range ordered magnetism and there is no measurable lattice modulation relating to a static CDW/SDW formation. Since the origin of the transition is unknown without a definite order parameter (OP) established for the emerging phase or for its characteristic elementary excitations, the term hidden order (HO) was adapted later on for the mysterious phase appearing at $T_o = 17.5$ K. Figure 2 illustrates the two dramatic, mean-field-like phase transitions in the specific heat. Note the large amount of entropy forming at T_o . The entropy $S = \int_0^{T_o} (\Delta C/T) dT$ is approximately $0.2 R \ln 2$ (R being the gas constant), and if magnetic, this result would indicate a very large contribution that should be detectable with magnetic neutron scattering.

The dc-magnetic susceptibility $\chi = M/H$ with $H = 2$ T is displayed in Fig. 3 for applied fields along the a and c axes. The magnetic response is strongly Ising-like, as there is only a magnetic signal along c which begins to deviate from a local-moment Curie-Weiss dependence below 150 K. The χ -maximum at ≈ 60 K indicates the coherence temperature T^* and the formation of a heavy Fermi liquid. The HO transition is hardly seen but it corresponds to the intersection of the drop with the plateau below 20 K (cf. Pfeleiderer et al. (2006)). Clearly the susceptibility of URu₂Si₂ is not that of a conventional bulk antiferromagnet. Nevertheless, there are several uranium compounds that do show a similar Ising-like behavior, for example, URhAl and UCo₂Si₂ (see, e.g., Sechovský and Havela (1998), Mihalik et al. (2006)).

Although the HO transition always occurs at 17.5 K and is robust, not dependent on sample quality, the low temperature properties are indeed sample dependent. Especially the resistivity $\rho(T)$ exhibits stronger decreases as the purity of the starting U material is increased. A characteristic plot of $\rho(T)$ for the two a and c directions in the body-centered tetragonal (BCT) unit cell of URu₂Si₂ (see below) is shown in Fig. 4. There is the negative temperature coefficient $d\rho/dT$ at high temperatures, followed by a maximum at ≈ 75 K, signaling the onset of lattice coherence, and then a dramatic drop to low temperatures and superconductivity. Presently one can find resistivity ratios of 500 or more with the best of today’s samples. The description of the high temperature resistivity ($T \gtrsim 100$ K) reaching $\approx 500 \mu\Omega\text{-cm}$ is open: either a strong Kondo-like scattering of incoherent, atomic U-spins takes place or, since the resistivity is above the Joffe-Regel limit, $k_F \ell \simeq 1$, (product of Fermi momentum and the mean-free path) variable range hopping occurs. As the local U-spins disappear

with the onset of coherence when temperature is lowered and the heavy-fermion state is created, the spin (fluctuations) scattering is removed and a coherent low-carrier state without significant scattering is formed. The superconducting transition temperature T_c varies significantly with sample quality and purity between 0.8 and 1.5 K and appears to coexist on a microscopic scale with the HO without disturbing it (Broholm et al., 1987; Isaacs et al., 1990).

Transport and thermodynamic measurements indicated a considerable Fermi surface (FS) reconstruction occurring at the HO transition (Maple et al., 1986; Palstra et al., 1985). The measured electronic specific heat in the HO and the jump in the resistivity at the transition are consistent with the opening of an energy gap over a substantial part of the FS. Maple et al. (1986) and Fisher et al. (1990) showed that the electronic specific heat in the HO can be extremely well described by $C_e(T) \propto \exp(-\Delta/k_B T)$, where Δ is the charge gap opening in the electronic spectrum below T_o . Fits to the measured C/T data gave $\Delta \approx 11$ meV and the gap was deduced to open over about 40% of the FS (Maple et al., 1986; Palstra et al., 1985). Subsequent resistivity (McElfresh et al., 1987) and Hall effect measurements (Schoenes et al., 1987) provided additional information on the opening of a gap at the HO transition. McElfresh et al. (1987) deduced from resistivity measurements a gap of about 7 meV, which, with hydrostatic pressure increased to about 10 meV. The early Hall effect experiments of Schoenes et al. (1987) clearly evidenced the opening of a gap in the HO, accompanied by a remarkable drop in the carrier concentration. These measurements also provided a rough estimate for the single-ion Kondo temperature, $T_K \approx 370$ K.

Thermal expansion experiments, $\alpha = L^{-1}(\Delta L/\Delta T)$, track the sample length L and hence the lattice constants a and c as a function of temperature surrounding the HO transition. The thermal expansion coefficient exhibits a large in-plane positive peak contrasting with the smaller negative one along the c -axis, both sharply peaked at T_o (de Visser et al., 1986). Hence, there is a net volume increase indicating a significant coupling of the HO to the lattice.

Because of the above conjectures of appearance of magnetism or CDW at the HO transition, neutron scattering (Broholm et al., 1987, 1991; Mason et al., 1990) and x-ray magnetic scattering (Isaacs et al., 1990) was brought to bear on the transition. By searching for scattering in directions where Bragg peaks were traditionally found in other compounds having the same ThCr_2Si_2 crystal structure with known long-range magnetic order, type-I antiferromagnetism was observed, with ferromagnetic $a - a$ planes, alternating antiferromagnetically along the c -direction (Broholm et al., 1987, 1991; Isaacs et al., 1990). Figure 5 illustrates the BCT ThCr_2Si_2 structure (space group $I4/mmm$) along with the putative antiferromagnetic type-I magnetic order on the U sublattice. Although magnetic Bragg peaks were found

at the proper \mathbf{Q} -values corresponding to the expected structure, there were particular difficulties with interpreting the neutron diffraction and x-ray Bragg peaks as conventional ordered-moment antiferromagnetism. i) The magnetic Bragg peak intensities were surprisingly small, corresponding to an ordered U moment of only $\mu_{\text{ord}} \approx (0.04 \pm 0.01) \mu_B/\text{U}$ (neutrons) and $\mu_{\text{ord}} \approx (0.02 \pm 0.01) \mu_B/\text{U}$ (x-rays). Muon spin rotation (μSR) measurements provided an ordered moment that was even an order of magnitude smaller (MacLaughlin et al., 1988). ii) The magnetic correlation lengths of about 400 Å are not resolution limited, i.e., the magnetic order is not truly long-ranged. iii) The measured temperature dependence of the neutron and Bragg intensities does not resemble a typical order parameter curve with its convex T-behavior. And iv) There are strong sample-to-sample variations of the Bragg peaks, when comparing their different temperature dependencies below T_o . So although the conventional wisdom proposed a Néel-type magnetic explanation even then around 1990 there were serious qualms about such a mundane interpretation.

Early inelastic neutron work drew particular attention to magnetic excitations appearing at low temperatures, which revealed that the inelastic neutron response of URu_2Si_2 differed markedly from that of, e.g., UBe_{13} and UPt_3 (Walter et al., 1986). Detailed neutron experiments were performed by Broholm et al. (1991) to detect the excitations or inelastic modes. They observed a continuous magnetic excitation spectrum, with two distinct gapped modes appearing at the antiferromagnetic wavevector $\mathbf{Q}_0 = (0, 0, 1)$ (equivalent to $(1, 0, 0)$) and at $\mathbf{Q}_1 = (1 \pm 0.4, 0, 0)$. Figure 6 shows the magnon energy-momentum dispersion determined by Broholm et al. (1991) overlaid with a full inelastic energy-momentum scan measured recently (Janik et al., 2009; Wiebe et al., 2007). The modes at $(0, 0, 1)$ and $(1.4, 0, 0)$ are commensurate and incommensurate, respectively, with the lattice. They sharply form at $T \lesssim T_o$ with gaps of about 2 to 4.5 meV, but, since the antiferromagnetic interpretation still prevailed in the early nineties, they were designated as ordinary magnon modes (Broholm et al., 1991). It was noted, though, that the antiferromagnetic mode was longitudinal and not transversal as is commonly expected for low-energy spin fluctuations. Thus the full meaning of these inelastic modes in the HO was a mystery and these modes are of intense attention today both experimentally and theoretically. Are they the elementary excitations of the HO state that cause this spin gapping? See Sec. IV below.

In order to determine the conductivity of URu_2Si_2 via a spectroscopic probe, the far-infrared reflectance has been measured by Bonn et al. (1988) as a function of frequency and temperature. Using an extended Drude model they track the optical conductivity into the coherence or heavy-fermion regime, characterized by the reduced scattering and enhanced effective mass, and further down below T_o where a partial charge gap opens. This result confirms that the FS is being reconstructed

in the transition to the HO state. Hence, combining transport, thermodynamic and optical data with those obtained from inelastic neutron scattering the HO state evidently possesses both a spin and a charge gap. Here we have the first clues of the microscopic HO behavior.

The enigmatic nature of the HO state became first recognized in the early nineties. The magnetic entropy $S_m(T)$ of URu_2Si_2 had been determined from the λ -type anomaly observed in the specific heat, see Fig. 2 (Maple et al., 1986; Palstra et al., 1985; Schlabitz et al., 1986), using $S_m(T) = \int_0^T (\Delta C/T') dT'$, where $\Delta C/T$ was obtained through subtracting the measured specific heat of ThRu_2Si_2 , which has no $5f$ electrons, from that of URu_2Si_2 . The entropy formed at T_0 was determined to be about $0.2 R \ln 2$ – a relatively large value (Fisher et al., 1990; Maple et al., 1986; Schlabitz et al., 1986). The magnetic entropy can be expressed as $R \ln(2S+1)$, or as $R \ln 2$, assuming that N uranium atoms have a $S = 1/2$ spin, i.e., a $1 \mu_B$ moment. It was noted that such a relatively large entropy change can, in particular, not be explained by assuming an antiferromagnetically ordered phase with small moments of only $0.04 \mu_B$ (see, e.g., Gor'kov and Sokol (1992); Ramirez et al. (1992); Walker et al. (1993)). Consequently, the detected small moment antiferromagnetism (SMAF) fails to account for the phase transition, and another, hidden order is responsible.

During the last two decades a quest for uncovering the HO arose. In these decades significant progress has been made in sample preparation and characterization. Superclean URu_2Si_2 samples were synthesized as well as samples with precisely controlled chemical substitutions. A wide variety of experimental probes were unleashed on the HO problem. Although our understanding about the HO has definitely increased, the HO proved itself thus far resistant. Concomitantly, many exotic theoretical models were proposed to explain the HO. Some of these could be dismissed while for others even the experimental techniques to verify or falsify them do not yet exist. Nonetheless, the most recent experiments provided more and clearer constraints for the theories whereby the multitude of mechanisms put forth for the HO could be narrowed down. Also, throughout these years, 1990 to 2010, significant progress was made in characterizing the unconventional superconducting properties through a variety of experimental probes. Experiments were carried out under pressure and with various dopings, both of which destroyed the HO and superconducting phases. The results of these studies have been nicely summarized by Pfeleiderer (2009) where the recent references are included.

III. WHAT IS HIDDEN ORDER

Hidden order evolves as a clear phase transition to a new phase at a temperature T_0 as determined from bulk

thermodynamic and transport measurements. Here the order parameter and elementary excitations of the new ordered phase are unknown, i.e., cannot be determined from microscopic experiments. In URu_2Si_2 all bulk quantities show a mean-field-like (2nd order) phase transition at 17.5 K, yet neutron and x-ray scattering, nuclear magnetic and quadrupole resonance (NMR, NQR), μSR , etc. are not able to reveal the OP and elementary excitations. We might mention four previous cases where the OP and elementary excitations were only uncovered many years after the experimental discovery: superconductivity, antiferromagnetism, 2D X-Y magnets and spin glass.

Basic properties of the HO state in URu_2Si_2 are i) the large reduction of entropy upon entering it, ii) the opening of charge and spin gaps, iii) a large decrease in the scattering rate along with a smaller effective mass, iv) greatly reduced carrier concentration, v) a clear coupling to the lattice, and vi) an electronically ordered state that can be destroyed by pressure, magnetic field and Rh-doping. Only out of the HO state evolves a highly unconventional (d -wave, even parity, spin-singlet) multi-gap superconducting ground state with $T_c \approx 1.5$ K (Kohori et al., 1996; Matsuda et al., 1996), being the focus of recent investigations (Kasahara et al., 2007, 2009; Matsuda et al., 2008; Morales and Escudero, 2009; Okazaki et al., 2008; Yano et al., 2008).

Now the question arises: Is the HO phase generic, i.e., can it, as defined above, be found in other materials with different types of interactions? And then once defined as HO, can it be unmasked and explained by known physical concepts and mechanisms? At present there is no comprehensive understanding of generic hidden order and its relation to quantum criticality. Nevertheless, the concept HO is beginning to make headway into the recent literature. For example, in the overview article of Coleman and Schofield (2005) it appears to mask the quantum phase transition in $\text{Sr}_2\text{Ru}_3\text{O}_7$ where a putative nematic phase has replaced the HO one. Recently the term HO and unidentified low-energy excitations were applied to the long-standing puzzle of the low-temperature phase transition in NpO_2 (Santini et al., 2006). In this case the “unmasking” of the HO was the identification of a staggered alignment of magnetic multipoles. Long-range ordering of electric or magnetic multipoles has to date only been unambiguously detected in a few materials, NpO_2 , UPd_3 , and $\text{Ce}_{1-x}\text{La}_x\text{B}_6$ being the most prominent examples. A review of HO as higher-rank multipolar (non-dipolar) driven phase transitions is given by Santini et al. (2009) and Kuramoto et al. (2009). A similar analogy can be drawn for the skutterudites, e.g. $\text{PrFe}_4\text{P}_{12}$ and $\text{PrOs}_4\text{Sb}_{12}$, where again a HO phase transition can be related to multipolar (quadrupole) ordering and compared to URu_2Si_2 (Hassinger et al., 2008a; Sato, 2008). In addition Dalla Torre et al. (2006) have used HO to describe a unknown phase in a 1D Bose insulator which exists between Mott and density wave phases; and Xu et al. (2007) used it for unidentified phases in a quantum spin fluid. Other areas to look for HO include the high tem-

perature superconductors (Valla et al., 2006). Here the nature of the pseudogap phase in the high-temperature cuprates has persisted as a major unsolved problem. Recent experiments have attempted to expose its “hidden order” (He et al., 2011). Finally, HO remains a possibility in the Ce-115 compounds (hidden magnetic order), the heavy fermions URu_2Si_2 and UPt_3 , various organic charge-transfer salts near the metal insulator transition, and non- or nearly magnetic oxides (Manna et al., 2010).

The term “hidden order parameters” was apparently first used in 1996 by Buyers who was then casting doubt that the measured small magnetic dipole transition was truly intrinsic and that conventional antiferromagnetism was the mediator of the phase transition at 17.5 K. Buyers additionally noted that inelastic neutron modes (spin excitations) were strongly involved in the HO transition. As $T \rightarrow T_o$ from below, the $\mathbf{Q}_0 = (0, 0, 1)$ mode softens and its damping increases thereby ruling out a crystal electric field (CEF) origin.

Shah et al. (2000) introduced the HO parameter in a Landau-Ginzburg free energy expansion which tried to describe the HO phase transition via two interacting order parameters Ψ , the primary unknown OP of the HO state, and m the magnetization as determined from neutron scattering/diffraction, as a secondary OP. Using such expansions Shah et al. (2000) were able to predict the magnetic field dependence of both Ψ and m and thereby determine the symmetry of the coupling between the two order parameters: $g\Psi \cdot m$ (bilinear) or $g\Psi^2 \cdot m^2$ (biquadratic).

These two scenarios were proposed for the two types of coupling posing the question: Does the Ψ order parameter break time reversal symmetry or not. The latter is possible, e.g. if Ψ would be related to a staggered electric quadrupolar order. Based upon the measured magnetic-field dependence of the neutron moment (Bourdarot et al., 2003a,b, 2005), the comparison favored the linear coupling scheme, thereby deducing that Ψ breaks time reversal symmetry. Consequently the HO would have a limiting constraint in its specific representation (Shah et al., 2000). However, while the above deduction was sound the question still remained: Is the small magnetic moment m tracked by the neutron scattering intrinsic to the HO? This conundrum plagued the field for many years and it became a point of contention and dispute. Only in recent years it has been fully clarified that the small antiferromagnetic moment is extrinsic, i.e., likely related to defects and stress in the sample. Early μSR measurements provided evidence for the existence of spatially inhomogeneous HO regions and antiferromagnetic ones; the latter occupied about 10% of the sample volume (Luke et al., 1994). Detailed ^{29}Si NMR studies (see below) supplied definite evidence for a spatially inhomogeneous development of antiferromagnetic regions with large moments of about $0.3 \mu_B$ (Matsuda et al., 2001). Further arguments against a homogeneous SMAF phase were derived from dilatation experiments (Motoyama et al., 2003), μSR (Amato et al., 2004), and recently, neu-

tron Larmor diffraction (Niklowitz et al., 2010). The tiny staggered moment of the putative SMAF phase originates thus from the smallness of the antiferromagnetic volume fraction, a scenario which was demonstrated by the fabrication of high-purity single crystals. In these high-quality samples the value of the detected small antiferromagnetic moment was brought down to $0.01 \mu_B$ and a clear phase boundary between the HO and an ordered large moment antiferromagnetic (LMAF) phase was observed (Amitsuka et al., 2007). Figure 7 compares the pressure dependence of the antiferromagnetic Bragg peak at $\mathbf{Q}_0 = (1, 0, 0)$ for a high-purity single crystal (labeled “present work”) with data obtained on older single crystals (labeled “previous work”) (Amitsuka et al., 2007).

IV. EXPERIMENTAL SURVEY

In 1999 Amitsuka et al. investigated the pressure dependence of the neutron magnetic Bragg peaks representing the small moment antiferromagnetism (SMAF), with $\mu_{\text{ord}} \approx 0.03 \mu_B$. Previous bulk resistivity measurements at pressures up to 1.5 GPa had shown little or no change in $\rho(T)$ or $d\rho/dT$ upon entering the HO phase. McElfresh et al. (1987) found only a slight increase of T_o as well as an increase of the transport gap. Surprisingly the Bragg-peak intensity at $\mathbf{Q}_0 = (1, 0, 0)$ exhibited a dramatic upturn at a pressure of 0.5 GPa. The corresponding ordered moment was $0.4 \mu_B$, a change of almost 15 (see Fig. 7). This reasonably large U-moment for a heavy-fermion material designated pressurized URu_2Si_2 to be the expected large moment antiferromagnet (LMAF) with a conventional magnetic phase transition at $T_N \approx 18$ K. Figure 5 displays the LMAF spin order. The neutron experiments were followed by pressure dependent ^{29}Si NMR probing the internal hyperfine fields in both the HO and LMAF states (Matsuda et al., 2001, 2003). These found evidence for a phase separation in the HO state of a few volume percent LMAF, which increased with pressure, thereby giving the “SMAF” response. It is now generally accepted that puddles of the LMAF are generated by stress field increasing the c/a axes ratio beyond a critical value (Yokoyama et al., 2005). This extreme sensitivity to sample quality, e.g., stress, impurities, etc. has been emphasized by Matsuda et al. (2008) who compared resistivity and specific heat data on samples cut from the middle with those on the surface of a high-quality single crystal. Figure 8 shows the now most up-to-date measurements of the $T - P$ phase diagram for URu_2Si_2 (Amitsuka et al., 2007; Niklowitz et al., 2010). Note the first-order phase transition separating the HO from the LMAF phase. Based upon the residual resistivity ratios a complete study of the crystal quality and various bulk properties has been carried out by Matsuda et al. (2011).

In order to probe the all-important Fermi surface in the HO phase of URu_2Si_2 quantum oscillations were studied, employing both de Haas-van Alphen (dHvA) and Shubnikov-de Haas (SdH) techniques (Altarawneh et al.,

2011; Hassinger et al., 2010; Jo et al., 2007; Nakashima et al., 2003; Ohkuni et al., 1999; Shishido et al., 2009). The early angular dependent dHvA measurements of Ohkuni et al. (1999) revealed three, rather small, closed FS pockets deep in the HO phase. This was once again consistent with a substantial FS gapping occurring in the HO phase. More recently, a larger, fourth FS sheet was found by SdH measurements on an ultraclean URu₂Si₂ sample (Shishido et al., 2009). Up-to-date angle-dependent SdH measurements revealed even a fifth branch, corresponding to a very small FS pocket (Altarawneh et al., 2011), as well as a previously unobserved splitting of one branch (Hassinger et al., 2010), see further Sec. VII below. The quantum oscillation measurements performed by different groups have provided data sets that are consistent with each other (cf. Hassinger et al. (2010)). Consequently, the FS of URu₂Si₂ in the HO has now definitely been established. The measured FS provides a stringent test for all theories of the HO. A full agreement with density-functional theory (DFT) calculations has only recently been achieved (Oppeneer et al., 2010). An interesting ingredient for the HO puzzle has come from dHvA and SdH measurements under pressure, which allow to probe the FS of the HO as well as of the LMAF phase. When pressure was applied to take the HO phase into the LMAF state, practically no change could be detected in the FS orbits as the pressure was increased to 1.5 GPa (Hassinger et al., 2010; Nakashima et al., 2003). The cyclotron effective mass decreased somewhat as expected for an increase in the magnetic moment. Accordingly, the FS with its partial gapping is not notably modified between the HO and LMAF phases. Consistent with this, the same FS nesting vector was detected by inelastic neutron experiments (Villaume et al., 2008). Hence, the FSs of the HO and LMAF phases are very similar, and furthermore these two distinct phases exhibit very similar transport and thermodynamical properties. This behavior has been termed “adiabatic continuity” (Jo et al., 2007), which however does not mean that these phases have identical OPs.

Since the quantum oscillations require a very low temperature, usually tens of milli-Kelvin, they cannot track the entrance into HO phase at 17.5 K. This warrants a description of the high temperature state out of which HO evolves. When the temperature is reduced below 100 K the incoherent local moment bearing U-ions have long since disappeared due to their hybridization with the *spd* electrons of the ligands. Now a coherent heavy-fermion state is formed which in recent nomenclature is termed the heavy-electron Kondo liquid (KL) (Yang et al., 2008). The characteristic KL temperature (coherence T^*) is ≈ 70 K in URu₂Si₂ as determined from a variety of bulk measurements. By lowering the temperature below T^* a correlation/hybridization gap is expected to partially open at the FS due to *f*-hybridization along this slow crossover into the KL. In heavy-fermion materials the KL should persist down to low temperatures (few Kelvins) where usually antiferromagnetic order or

superconductivity occurs. However, in URu₂Si₂ already at 17.5 K the HO transition takes place with striking FS reconstruction and gapping.

Figure 9 collects three transport properties as the temperature is reduced from the paramagnetic KL through the HO into the superconducting state (Kasahara et al., 2007). There is a continuous drop in the resistivity in the HO despite the loss of carriers as exemplified by the large jump in the Hall coefficient $R_H \propto 1/n$, the carrier concentration. Since $\rho = m^*/(e^2 n \tau)$, the scattering rate $1/\tau$ must dramatically decrease to compensate for the reduction in n . Note the large residual resistivity ratio of 670 for the high quality URu₂Si₂ crystal used. The effective mass m^* is not expected to vary significantly in this temperature region. The magnetoresistance $\Delta\rho(H)/\rho(0)$ is very large and proportional to H^2 , meaning that URu₂Si₂ is a compensated electron - hole semimetal, i.e., $n_e \approx n_h$ (as was noted originally by Ohkuni et al. (1999)). Further analysis of the Hall data gives a hole concentration of ≈ 0.10 holes per U atom in the paramagnetic KL (Oh et al., 2007) which becomes 0.02 holes per U atom in the HO (Kasahara et al., 2007). It is remarkable that superconductivity can occur at such low carrier concentration.

The thermal electricity of URu₂Si₂ is also unusual (Bel et al., 2004). There are clear indications of the HO transition from the Seebeck coefficient (thermoelectric power) and an unusually giant Nernst effect (ratio of transverse electric field to longitudinal thermal gradient). These effects confirm the drastic decrease in the scattering rate and the low density of itinerant electrons that carry a large entropy.

Another transport property, the thermal heat conductivity κ , displays a steep increase upon entering the HO state from the KL (Behnia et al., 2005; Sharma et al., 2006). Since there are two contributions to κ one must separate the phonons (κ_p) from the electrons (κ_e). As the Wiedemann-Franz law is not fully valid here, the thermal Hall (or Righi-Leduc) conductivity κ_{xy} is used to independently determine κ_e . The electronic contribution is found to be extremely small with the phonons carrying most of the thermal conduction. This signifies the large FS gap opening at T_o which greatly decreases the electron-phonon scattering. By analyzing κ in terms of the mean-field Bardeen-Cooper-Schrieffer (BCS) model, one obtains a strong coupling of the HO with its itinerant electrons to the lattice, i.e., $2\Delta(T=0)/k_B T_o \approx 8$ (Sharma et al., 2006). The applicability of an itinerant model to describe the κ -data has been used to suggest a density wave scenario with strong lattice coupling (Sharma et al., 2006). However, despite various attempts to find periodic lattice distortions, none have been found. Solid state probes that are sensitive to the local symmetry like NMR/NQR would be able to detect these, but none have been found (Saitoh et al., 2005).

The elastic properties of URu₂Si₂ have been measured with ultrasonic techniques (Kuwahara et al., 1997; Wolf et al., 1994). A softening is observed in the c_{11} and transversal $(c_{11} - c_{12})/2$ modes at temperatures below

~ 70 K, marking the onset of the coherence temperature (Kuwahara et al., 1997). The elastic anomalies observed at T_o are in contrast quite small, indicating that no uniform distortion occurs at T_o . The longitudinal c_{11} shows a broad minimum at 30 K and increases slightly ($\sim 0.1\%$) when temperature is lowered (Kuwahara et al., 1997; Wolf et al., 1994).

Point-contact spectroscopy (PCS) measurements at temperatures around T_o have been applied to detect the opening of a conductance gap in the HO state (Escudero et al., 1994; Hasselbach et al., 1992; Morales and Escudero, 2009; Rodrigo et al., 1997; Thieme et al., 1995). All PCS data generally evidence the opening of such gap, however, its onset is consistently found at about 19–25 K and not at T_o . As explained by Rodrigo et al. (1997) the pressure that is exerted to drive the point-contact in the surface causes locally a shift of T_o to a higher value. PCS measurements at higher temperature detected the onset of a resonance structure at the Fermi level starting at $T \approx 60$ K, consistent with the opening of a coherence/hybridization gap at T^* (≈ 70 K) derived from bulk Hall and resistivity measurements (Palstra et al., 1986; Schoenes et al., 1987). Morales and Escudero (2009) applied PCS to the superconducting state to probe the superconducting gap below $T_c = 1.5$ K. They observe this gap, but unexpectedly and unexplained, its temperature dependence does not follow a BCS-type shape and its onset starts already above T_c .

Resistivity studies under pressure were performed by Jeffries et al. (2007, 2008) and Motoyama et al. (2008), who tracked the evolution of the charge gap from the HO into the LMAF. The transport gap was found to increase, when crossing from the HO to the LMAF, with the HO gap being about 70% to 80% of the LMAF gap. Also a kink in the critical temperature was detected when passing from T_o to T_N under pressure.

Inelastic neutron scattering (INS) redux was carried out by Wiebe et al. (2007) at temperatures spanning the HO transition. The authors tracked the commensurate $\mathbf{Q}_0 = (1, 0, 0)$ and incommensurate $\mathbf{Q}_1 = (1.4, 0, 0)$ modes to higher energies and temperature. The characteristic gap energies of 2 and 4 meV of these sharp spin waves were found in the HO phase. Above T_o the \mathbf{Q}_0 mode transforms to weak quasielastic spin fluctuations. In contrast the \mathbf{Q}_1 mode is due to fast, itinerant-like, well-correlated spin excitations reaching energies up to 10 meV, i.e., a continuum of excitations. The authors relate these incommensurate spin fluctuations to the heavy quasiparticles that form below the coherence temperature T^* with a corresponding increase in entropy. The gapping of such strong spin fluctuations was related by Wiebe et al. (2007) to the loss of entropy at the HO transition. By analyzing the spectrum for $T > T_o$ the specific heat could be estimated along with the entropy loss. The calculational relationship between the spin excitation gapping and the Fermi surface gap establishes the strong coupling between spin and charge degrees of freedom for this collection of itinerant electrons. Therefore,

the HO can be viewed as a rearrangement of electronic states at the Fermi energy, giving rise to the gapping of these two coupled but distinct types of excitations. Yet the mechanism of the HO or “driving force” causing the gapping and the electronic rearrangement remain unknown (Wiebe et al., 2007). As noted here, in accordance with earlier neutron studies, no CEF excitations were found up to 10 meV.

Further INS experiments examining the intriguing inelastic modes behavior were carried out in Grenoble (Villaume et al., 2008). Here the pressure and temperature dependence of the \mathbf{Q}_0 commensurate mode was determined as the HO was entered from above. With pressure \mathbf{Q}_0 transforms from an inelastic excitation to a normal magnetic Bragg peak in the LMAF, i.e., the longitudinal spin fluctuations “freeze” and become the static long-range antiferromagnetic order, with $\mu_{\text{ord}} \approx 0.4 \mu_B$. In contrast the incommensurate \mathbf{Q}_1 mode persists as inelastic to the highest pressures with an increase in its energy. $\mathbf{Q}_1 = (1.4, 0, 0)$ represents thus a FS nesting vector found in both the HO and LMAF phases. Conversely, the antiferromagnetic mode at \mathbf{Q}_0 is a true signature of the HO (Villaume et al., 2008). The T – P phase diagram extracted from the neutron scattering supplemented by thermal expansion and calorimetric data (Hassingier et al., 2008b) is similar to that shown in Fig. 8. Hence, one can now follow the intensity of the antiferromagnetic spin fluctuations at \mathbf{Q}_0 out of the KL into the HO.

Very recently a detailed study of the (polarized) inelastic neutron resonances at \mathbf{Q}_0 (and \mathbf{Q}_1) was performed by the Grenoble group focusing on the commensurate antiferromagnetic resonance at $(0, 0, 1)$ (Bourdarot et al., 2010). The dynamical spin susceptibility $\chi(\mathbf{Q}, \omega, T)$ that is related to the spin-spin correlation function was determined and analyzed above and below T_o . Clear spin correlations at \mathbf{Q}_0 were observed as the temperature was scanned through T_o with a jump in the resonance energy or spin-gap energy E_0 and a BCS-like T-behavior of the integrated imaginary susceptibility, see Fig. 10. It was predicted by Elgazzar et al. (2009) that the integrated spin-spin correlation function should display OP behavior. It thus appears that the \mathbf{Q}_0 spin resonance is a main signature of the HO phase. As proposed by Wiebe et al. (2007) the incommensurate \mathbf{Q}_1 mode that appears in both the HO and LMAF phases accounts for a large share of the loss of entropy due gapping of the mode and corresponding loss of spin fluctuations. A major question is how the spin gap is connected to the charge gap of the FS. Is the spin resonance at the antiferromagnetic wavevector driven by the electronic gapping of the FS, or *vice versa* is the spin resonance responsible for the FS gapping? In order to explain the observed behavior Bourdarot et al. (2010) suggest that that both itinerant and local $5f$ electrons are playing a role, with itinerant electrons responsible for the spin gaps and localized electrons for the FS gap, thereby requiring a duality interpretation. Figure 11 collects the various energy scales for the neutron resonances and compares them with the gap energies

from bulk resistivity measurements. Note the step-wise increase of the charge gap Δ_G at the HO–LMAF phase transition. The spin gap E_1 of the incommensurate mode also step-wise increases, whereas the commensurate mode with gap E_0 vanishes in the LMAF.

So with this collection of sophisticated experiment on ever improving crystal quality, what have we learned about HO? We will now give a brief summary to conclude this section.

HO is not a magnetic dipole (local-moment) ordered transition and ground state. Yet as with all strongly correlated electron systems magnetism hovers in the background, every ready to make an appearance, in our case as dynamical spin excitations. The salient features of the HO are the pronounced Fermi surface reconstruction and gapping at T_o . Surprisingly, there is practically no change in the FS properties between HO and LMAF. The high-T phase out of which HO appears can be designated as the recently proposed Kondo liquid (Yang et al., 2008). This raises the question as to the exact nature of a Kondo effect in URu₂Si₂. Above T_o a correlation/hybridization gap slowly opens in the coherence crossover regime, its importance has up till now been neglected. The FS topology of URu₂Si₂ in the HO has now been determined to consist of only relatively small, closed pockets. The HO ground state is that of a very low carrier concentration, compensated semimetal with strong lattice coupling. Itinerant electrons appear to be the main characters here as most experimental evidence supports an itinerant electron or band-like scenario. There is no “smoking gun” for a localized uranium $5f^2$ or $5f^3$ configuration (see Oppeneer et al. (2010) for a discussion of this issue).

The INS has given us two modes or resonances: Pre-eminent is the \mathbf{Q}_0 commensurate resonance which mimics OP behavior of the HO state. The \mathbf{Q}_1 incommensurate spin mode, present in both the HO and LMAF phases, could be responsible for the similar loss of entropy at T_o in HO and at T_N in LMAF (Balatsky et al., 2009; Wiebe et al., 2007). There is an intimate relationship between charge and spin degrees of freedom. A special charge-spin duality or coupling seems to exist here analogous to what is now fashionable in the topological insulators, where a similar charge-spin duality comes into play (Hasan and Kane, 2010). Nevertheless, the driving force or mediator for creating the HO transition remains to be clarified.

V. THEORETICAL SURVEY

There have been a large number of theoretical contributions to the HO problem spanning the past 25 years. We review these here and attempt to relate them to the present experimental developments.

The earliest theoretical models focussed on explaining the unusually small ordered moment and its Ising-like behavior that had been found in the neutron scattering and susceptibility experiments (Broholm et al., 1987; Palstra

et al., 1985). A first CEF model for URu₂Si₂ was developed by Nieuwenhuys (1987), who considered a $U^{4+} 5f^2$ ion with total angular momentum $J = 4$ in a tetragonal crystal field. He showed that a reasonable agreement with experimental susceptibility data could be obtained when the three lowest CEF levels would be singlets with a splitting of about 40 K between the ground and first excited state ($|\Gamma_1^{(1)}\rangle = \alpha(|4\rangle + |-4\rangle) + \beta|0\rangle$ with $2\alpha^2 + \beta^2 = 1$ and $|\Gamma_2\rangle = (|4\rangle - |-4\rangle)/\sqrt{2}$, respectively). The predicted ordered moment was however ten times larger than the measured one.

Two early on theoretical models began to treat the HO phase beyond the simple small-moment antiferromagnetic ordering. To explain non-Néel magnetically ordered phases characterized by weak antiferromagnetism Gor’kov (1991) and Gor’kov and Sokol (1992) proposed double ($\langle S_\alpha(r_1)S_\beta(r_2) \rangle$) and triple ($\langle S_\alpha(r_1)S_\beta(r_2)S_\gamma(r_3) \rangle$) spin correlators as driving order parameter which break spin rotational symmetry, yet the local magnetization is zero. Here the spins can be on different U ions or on the same U ion, in which case the spin correlators are equivalent to quadrupole or octupole moments. Ramirez et al. (1992) analyzed the nonlinear susceptibility and proposed a double-spin correlator, that would give rise to a staggered quadrupolar order.

Walker et al. (1993) performed angular dependent *polarized* neutron scattering to search for higher order spin correlators and spin nematic order parameters. A substantial neutron spin-flip scattering was observed, which was interpreted as evidence against a spin nematic or quadrupolar magnetization distribution. Various higher order multipoles could be excluded as well. It is however a question in how far these measurements were influenced by a parasitic SMAF phase. As a test of the proposed non-Néel orders Barzykin and Gor’kov (1993) predicted that there should exist broken-symmetry Bragg peaks for spin nematic and triple-spin correlator phases that could be induced with an external magnetic field. Neutron experiments searching for such a field dependence were undertaken but gave a null result, thereby discarding these theories (Buyers, 1996; Mason et al., 1995).

An extensive CEF treatment was developed by Santini and Amoretti (1994), who considered the same U^{4+} CEF Hamiltonian as Nieuwenhuys (1987), but analyzed in detail the possible energetic orderings of the nine CEF states and considered different angular momentum operators that can support multipolar order parameters. They observed that there exist three possible variants for the three lowest singlet levels. The first variant (A), that was considered by Nieuwenhuys (1987), could support dipole order (J_z) simultaneously with hexadecapole order ($J_x J_y [J_x^2 - J_y^2]$), but this variant was rejected because it would give a much too high Schottky contribution to the specific heat. The other two variants (B and C) could both sustain a quadrupole ($J_x J_y$ or $(J_x^2 - J_y^2)$) and an octupole ($J_z (J_x^2 - J_y^2)$ or $J_z J_x J_y$) order parameter. Based on a comparison with experimental data Santini and Amoretti (1994) favored electric quadrupolar order-

ing of localized f electrons for the HO. The dipole matrix elements would be zero for these two variants, but they suggested that a small static dipole magnetic moment could be induced by quadrupolar ordering. Walker and Buyers (1995) however noted that dipole order cannot be induced as a secondary OP by quadrupolar order and that the proposal would not be compatible with the polarized neutron scattering (see also Santini (1998); Santini and Amoretti (1995)). As mentioned before, there is to date no experimental evidence of such localized CEF levels and splittings.

A different CEF interpretation was proposed by Barzykin and Gor'kov (1995) who suggested that U ion could be in an *intermediate valence* configuration, dominantly U^{4+} , but with a small admixture of half-integer spin configurations ($5f^1$ or $5f^3$) being responsible for the small moment.

The first suggestion of an itinerant-localized duality model was made by Sikkema et al. (1996), who developed an Ising-Kondo lattice model, in which they adopting the U^{4+} two singlet CEF level ground state (variant A) with additional on-site exchange coupling to the conduction electron spins, leading to Kondo screening. In this model the HO is explained as small moment antiferromagnetism, but the appearance of such a state is now regarded as being parasitic to the HO. Another itinerant-localized duality model was suggested by Okuno and Miyake (1998). They used an induced-moment mechanism for the SMAF appearing from a singlet-singlet CEF scheme along with a partially nested FS of the itinerant electrons. Accordingly, the SMAF is found to be compatible with the large specific heat jump and is composed of both spin and orbital components. While the duality model is also employed in more current HO theories, see for example Tripathi et al. (2005), here it is focused on explaining the SMAF which is now believed to be extrinsic.

Kasuya (1997) proposed that the HO would be due to dimerization on the U sublattice. Here the corresponding atomic displacements should be observable with x-ray diffraction or extended x-ray absorption fine structure (EXAFS) but have never been detected.

Another novel starting point for the HO transition is the unconventional spin density wave (SDW) theory by Ikeda and Ohashi (1998). In this model the electron-hole pair amplitude changes its sign in momentum space. For the d -wave superconductors this is called a d -density wave (DDW). Using a mean-field extended Hubbard model, the energy gap and thermodynamic properties can be calculated. They exhibit a sharp specific-heat cusp, a clear drop in the uniform susceptibility and a zero staggered magnetization. Except for the susceptibility the above temperature dependence agree with experiment. However, a microscopic signature of the DDW has not yet been found. Presumably an ARPES measurement would be able to detect the FS modulation in k space. A modern extension of the DDW model is the chiral DDW of Kotetes and Varelogiannis (2010)

and Kotetes et al. (2010) who demonstrate that a chiral ground state could be responsible for the anomalous thermoelectric and thermomagnetic effects (e.g., Nernst effect) in URu_2Si_2 .

As mentioned above, different CEF schemes can be adopted for the U^{4+} ion. Experiments performed on diluted $U_xTh_{1-x}Ru_2Si_2$ with $x \leq 0.1$ (see below) were interpreted as an indication of a *doublet* CEF ground state (Amitsuka and Sakakibara, 1994). If the $5f^2$ CEF ground state is assumed to be a non-Kramers Γ_5 doublet ($|\Gamma_{5\pm}\rangle = |\gamma| \pm 3\rangle + \delta|\mp 1\rangle$, $\gamma^2 + \delta^2 = 1$) in stoichiometric URu_2Si_2 as well, different multipole characters could become possible. Ohkawa and Shimizu (1999) considered the Γ_5 doublet and from a consideration of angular momentum matrix elements proposed that a magnetic dipole or a non-magnetic quadrupole can be formed. Depending on the fine tuning (e.g., pressure) one can transform one ground state into the other. So within this local CEF scheme the HO and the LMAF phases are explained as quadrupolar and spin-dipolar ordering, respectively. Once again, the local CEF levels have never been experimentally observed – they should be hybridized away in a KL. Yet, based upon an analysis of the dHvA amplitude (Ohkuni et al., 1999) as a function of magnetic field orientation a series of 16 nodes appear. This behavior can be related to an Ising degree of freedom in the U^{4+} electronic configuration, that would be possible with a Γ_5 doublet. According to Silhanek et al. (2006b) the local Γ_5 doublet becomes hybridized with the conduction electrons and itinerant quasiparticle bands having Γ_5 character are formed via this hybridization. This model then proposes itinerant antiferro quadrupolar order for the HO. Although such electrical quadrupoles could be detectable with resonant x-ray scattering (RXS) they have thus far not been observed (Amitsuka et al., 2010; Walker et al., 2011).

Yamagami and Hamada (2000) proposed that the HO could be an antiferromagnetic phase with a small magnetic moment caused by cancellation of a large spin and an equally large but antiparallel orbital moment. Neutron form factor measurements would be able to detect this, but could not confirm this effect (see, e.g., Broholm et al. (1991); Kuwahara et al. (2006)).

Within the basic ingredients of a heavy Fermi liquid, Chandra et al. (2002) proposed that the HO in URu_2Si_2 resulted from *incommensurate* orbital antiferromagnetism associated with circulating charge currents between the U-atoms. The model was based upon the appearance of a weak internal field below T_0 detected by the ^{29}Si NMR line-width broadening (Bernal et al., 2001). These plaquette currents cause an orbital moment to form, thereby breaking time reversal symmetry, that can be estimated from the isotropic field distribution at the Si sites. Thus the HO order parameter is taken to be proportional to the temperature onset of the line-width broadening. Chandra et al. (2002) calculated the local fields and the large entropy transition in the specific heat, and detailed predictions were made to relate the in-

commensurate current ordering to the neutron-scattering cross-section. A ring of scattering intensity was forecast at a specific anisotropic \mathbf{Q} -radius which was experimentally sought but not found (Wiebe et al., 2004). In addition the NMR line-width broadening was found to be much reduced when higher quality stress-free single crystals were investigated (Bernal et al., 2006; Takagi et al., 2007).

Scenarios for higher-order multipolar transitions were put forward by Kiss and Fazekas (2005) and Fazekas et al. (2005). By assuming an itinerant to localized transition upon entering the HO phase from above, Kiss and Fazekas (2005) treated the HO state as multipolar orders via symmetry-group theoretical arguments. Within the 3-singlet CEF model, $U^{4+} - 5f^2$ ions can carry a sequence of higher multipole order parameters. The authors thereby consider a manifold of multipolar order parameters spanning the gamut from magnetic dipoles (rank 1) to magnetic triakontadipoles (rank 5). Led by the time-invariance breaking detected by neutrons (Bourdarot et al., 2003a; Walker et al., 1993), by NMR (Bernal et al., 2001, 2006), and μ SR (Amato et al., 2004) they propose staggered octupolar order for the HO, which would be time-reversal symmetry breaking and have a vanishing total dipolar moment. Further arguments were based on comparisons with uniaxial stress measurements, from which they concluded that a triakontadipole (which also breaks time-reversal symmetry) would be incompatible with the uniaxial response to stress. Notably, Fazekas et al. (2005) predict the onset of octupolar order at T_0 , followed by a second transition due to quadrupolar ordering at $T \approx 13.5$ K. While this theoretical conjecture is most intriguing, the observation of multipoles of rank higher than two is experimentally hardly accessible. Also, there is little evidence for another transition below T_0 . Nevertheless this work has inspired a succession of additional theoretical efforts directed toward higher-order multipoles. Hanzawa and Watanabe (2005) adopted a singlet-doublet CEF level scheme and deduced that $J_x(J_y^2 - J_z^2)$ octupolar order would be most probable. *Incommensurate* ordering of octupoles was suggested by Hanzawa (2007). Very recently, an antiferro ordering of time-even hexadecapoles was proposed as HO parameter by Haule and Kotliar (2009) and a ferromagnetically aligned ($\mathbf{Q} = 0$) time-odd triakontadipolar HO parameter was proposed by Cricchio et al. (2009). Antiferro-quadrupole order of $J_x J_y$ -type was proposed by Harima et al. (2010), and antiferro-hexadecapolar ordering of $xy(x^2 - y^2)$ type was proposed by Kusunose and Harima (2011). A full review of multipole orders in strongly correlated electron systems has recently been given by Santini et al. (2009) and Kuramoto et al. (2009).

A serious drawback of the CEF multipolar theories is that these from the outset assume a localized $5f^2$ configuration, but as mentioned before, there is no experimental evidence for such localized CEF levels and splittings. Moreover, recent resonant x-ray scattering experiments sought for quadrupolar order but could not

observe it (Amitsuka et al., 2010; Walker et al., 2011). This would thus exclude any quadrupole scenario. Also as discussed by Walker et al. (2011) the magnetic form-factor of URu_2Si_2 is normal, which would exclude magnetic octupolar and triakontadipolar orders. Conversely, previous RXS measurements on established multipolar ordered materials did, for example, unambiguously detect non-collinearly staggered quadrupole order in NpO_2 , $Ce_{1-x}La_xB_6$, and UPd_3 (see Paixão et al. (2002), Walker et al. (2006), and discussions provided by Kuramoto et al. (2009); Santini et al. (2009)). Also, NMR measurements have been shown to be able to detect quadrupolar symmetry breaking in NpO_2 (see, e.g., Tokunaga et al. (2005)), although it could be that contributions cancel out in URu_2Si_2 . An often neglected aspect of CEF theories is that they do offer insight in the possible multipole symmetries on a single U ion, but this is not sufficient to achieve collective long-range order, which requires a mechanism providing exchange coupling of multipoles. Investigations of the multipolar exchange interaction are only in their initial phase (cf. Suzuki et al. (2010)). Lastly, while thus far all CEF theories assume a U^{4+} ion, a recent electron energy loss spectroscopy (EELS) study determined a $5f$ occupation of 2.7 (Jeffries et al., 2010), which is not close to a $5f^2$ configuration. The EELS result, combined with a magnetic entropy approaching $S_{mag} \sim R \ln 4$ at high temperatures (Janik, unpublished, 2008), would rather suggest a Kramers $5f^3$ ion to be realized at high enough temperatures. As mentioned before at low temperatures itinerant f character appears to prevail.

Helicity order, i.e., the establishment of a fixed axis of quantization for the spins on the FS, was proposed as the HO cause by Varma and Zhu (2006). Such order arises when the Pomeranchuk criteria for the spin-antisymmetric Landau parameters are violated with respect to the Fermi-liquid state. In order to remove or “cure” this instability a nematic phase transition occurs thereby creating the HO phase. For URu_2Si_2 this model represents a displacement of the FS into up and down sheets. Based upon the then-known band structure and FS, and variations of the density of states near the FS, Varma and Zhu (2006) calculated different experimental features: specific heat, linear and non-linear susceptibilities, and the NMR line-width broadening. Using the properly modified Landau parameters good agreement with the data was found. The main difficulty with this approach is the neglect of the exact, complex FS and its significant hot spot gapping upon entering the HO state. Also, as spin-orbit coupling is strong in uranium, a picture of pure spin up and down states is not sufficient. Positron annihilation was employed to study FS changes in the HO, but could not confirm helicity order if this state would form as a single domain (Biasini et al., 2009). Up until now the suggested microscopic experimental verifications (Varma and Zhu, 2006) of the helicity order have not been accomplished.

By way of relating the HO transition to a SDW Mineev

and Zhitomirsky (2005) employed a double dual approach whereby two order parameters Ψ and m were considered. In addition there were also two subsystems: local CEF moments on the U^{4+} sites along with conduction electrons in nested bands. Strong electron-electron interactions were added to drive the SDW in a commensurately nested FS. The SDW then induces a local SMAF or m in the HO state. Ψ represents the SDW amplitude and is the primary order parameter which governs the experimental behavior. The pressure dependence is predicted to show a line of first-order transitions ending in a critical end-point that separates the SMAF from the LMAF. The high magnetic field properties are calculated from the model to account for the multiple phases (See Sec. VI). Unfortunately experiment does not find a SDW even with a small form factor and it is now commonly accepted that the SMAF is extrinsic, and instead of a critical end-point there is the merging of all three phase lines at a bicritical point (Amato et al., 2004; Amitsuka et al., 2007; Hassinger et al., 2008b; Motoyama et al., 2003; Niklowitz et al., 2010). Figure 8 presents the up-to date pressure-temperature phase diagram for URu_2Si_2 . Note the three distinct phases: KL, HO and LMAF. The SMAF is omitted since it is extrinsic.

VI. HIGH MAGNETIC FIELDS AND Rh-DOPING

There were various pioneering attempts to study the high magnetic-field H behavior of URu_2Si_2 in the HO state and beyond by de Boer et al. (1986) and Sugiyama et al. (1990). Such experiments showed the destruction of the HO phase transition with fields approaching 35 T and the occurrence of novel phases between 35 and 42 T. However, the use of short-time (<1 ms) pulsed fields resulted in a loss of temperature equilibrium for these highly conducting samples and the $T - H$ phase diagram was unclear. Here the field H is applied along the tetragonal c -axis, with little or no magnetic response for fields in the basal plane.

More recent investigations began in 2002 with continuous H -fields reaching 45 T for specific heat, magnetocaloric effect (MCE), and magnetoresistance (Jaime et al., 2002; Kim et al., 2003a). These measurements detected the suppression of the HO phase at 35.9 T (H_0), the appearance of a new phase between 36.1 T (H_1) and 39.7 T (H_2) with no additional phase transition above 40 T. While the low field HO transition in the specific heat is λ -like (second-order), with increasing field its shape changes to a symmetric peak indicating a first-order transition. The new high-field phase is always reached through a first-order transition. The above results are confirmed via the MCE, which uncovers an increase in the magnetic entropy at H_0 , a drop in S_{mag} at H_1 , concluding with a final entropy rise above H_2 . The magnetoresistance also established this three-step behavior.

Long-time pulsed (>100 ms) magnetic fields were

brought to bear for magnetization experiments reaching 44 T at 0.5 K (Harrison et al., 2003). These measurements revealed that the HO phase is destroyed before the appearance of the reentrant phase between 36 and 40 T. At temperatures above the maximum in the “novel” phase, ≈ 6 K, the magnetization and susceptibility (dM/dH) indicate an itinerant electron metamagnetism, i.e., an ever-sharpening peak in the susceptibility which disappears at the reentrant transition. Yet extrapolation of its T -dependence through the novel phase suggests a quantum-critical end point at 38 T. Thus a putative quantum critical point is overpowered by the formation of the novel phase.

Further experiments to examine this magnetic-field-induced critical point were carried out by Kim et al. (2003b) via a comprehensive magneto-resistivity study. By plotting continuous variations of $\rho(H)$ at various temperatures and $\rho(T)$ at various fields, the extremities in $d\rho/dH$ and $d\rho/dT$ were determined; and by combining these results with the above findings, a complete $T - H$ phase diagram could be constructed. Figure 12 exhibits this high-field phase diagram with the details of the five distinct phases three of which are the newly discovered novel phases.

Recent measurements of quantum oscillations in the resistivity, i.e., the Shubnikov-de Haas (SdH) effect, by Jo et al. (2007) demonstrated the dramatic reconstruction of the Fermi surface when leaving the HO phase and entering phase II (orange in Fig. 12) spanning the fields region around 35 T. The SdH results suggest an increase in the effective carrier concentration thereby destabilizing the gapping of the itinerant quasiparticles which leads to the increase in the magnetization. The high-field sweeps were also performed under pressure beginning in the LMAF phase and field-driven to novel phase formation. Here the high-field phases determined by resistivity show qualitatively the same number and $T - H$ shapes as the ambient pressure phases. This means that pressurizing the material from HO to LMAF does not alter the resulting high-field phase formations, again indicating the similar FSs in HO and LMAF. The high-field Fermi surface reconstruction was further indicated from a combination of resistivity, Hall and Nernst effect measurements (Levallois et al., 2009).

The effect of Rh-doping allows us to simplify the high-field phase diagram. It has been known for since the early work of Amitsuka et al. (1988) that small amounts of Rh substituted for Ru create puddles of LMAF and suppress the HO via a combination of stress at the larger Rh-sites and the addition of an extra $4d$ electron. Above 4 percent Rh substitution on the Ru site both HO and LMAF are removed; and there is only a heavy Fermi liquid (HFL) ground state in low fields, i.e., no ordered phase of any kind. A large magnetic field has been applied to study its effect on the HFL. Kim et al. (2004) carried out a systematic study of Rh substitution in $U(Ru_{1-x}Rh_x)_2Si_2$ in fields up to 45 T. The complicated five phases were reduced at $x = 0.04$ to a single field-induced phase: The

surviving symmetric dome-like shape of phase II (orange in Fig. 12) spans the field 26 to 37 T with a maximum peak temperature of 9 K. By extrapolating the HFL-behavior of the resistivity and magnetization data from outside the dome to inside, a single point is reached at 0 K and 34 T, again suggesting a field-induced quantum critical point that is suppressed by the formation of a field-induced novel phase. Further analysis of the 4 percent Rh doped samples, $\text{U}(\text{Ru}_{0.96}\text{Rh}_{0.04})_2\text{Si}_2$, was carried out by Silhanek et al. (2005, 2006a) using specific heat and magnetocaloric measurements. Here the high-field novel phase II was mapped out and comparisons drawn with the valency transition in $(\text{Yb}_{1-x}\text{Y}_x)\text{InCu}_4$ and the metamagnetic transformation in CeRu_2Si_2 . Figure 12 also compares the $H - T$ phase diagram for $\text{U}(\text{Ru}_{0.96}\text{Rh}_{0.04})_2\text{Si}_2$ with that of undoped URu_2Si_2 . Recently a theoretical description of the suppression of HO by Rh impurities was presented by Pezzoli et al. (2011). They studied the local competition of HO- Ψ with LMAF- m where disorder is the driving force of the two competing effects. Accordingly, the phase diagram as a function of x-Rh is obtained and compared with the local LMAF “patch” model derived from ^{29}Si NMR (Baek et al., 2010).

Another way of slowly quenching the HO with doping is to substituted Re for Ru. A recent study (Butch and Maple, 2009) has found that ≈ 15 percent Re substitution leads to a ferromagnetic phase beginning at a putative quantum-phase transition. This work suggests the possible formation of a ferromagnetic quantum-critical point.

A final aspect of doping the pure URu_2Si_2 compound is to reduce the U concentration to the dilute limit, i.e., $\text{R}_{1-x}\text{U}_x\text{Ru}_2\text{Si}_2$ where $\text{R} = \text{Th, La; Y}$ and x is a few percent U. Such investigations were pioneered by Amitsuka and Sakakibara (1994) and spanned a decade of experimentation (Yokoyama et al., 2002). The important questions posed here are: Can dilute U in a non-magnetic matrix support a single-impurity Kondo effect or even a multichannel Kondo behavior (Cox, 1987)? Are the $5f$ electrons of the single-ion U localized and magnetic with a Kondo effect or itinerant - dissolved into the conduction density of states at E_F ? As is well-known in Kondo physics it would seem that this depends on the particular matrix, Th, La, or V (Marumoto et al., 1996). The conclusion after many measurements was however ambiguous, neither of the above two possibilities – conventional or multichannel Kondo effect – were clearly established. Presently this topic has gained renewed interest from both the theoretical and experimental sector (Toth et al., 2010).

VII. PRESENT STATE OF HO

There persists particularly strong interest today in solving the HO enigma. At present (January 2011) experiment has turned towards repeating some of the previ-

ous (20 year old) measurements using the latest advances in experimental methods and crystal growth as, for example, with the aforementioned INS (Bourdarot et al., 2010). Here we consider first the recent progress made in optical conductivity and quantum oscillations. Further experimentation has taken advantage of techniques developed for and effectively utilized in the high temperature superconductors, *viz.*, STM/STS and ARPES which we discuss below. A surge in new theories dedicated to the HO is simultaneously taking place; their current status is surveyed below.

Optical conductivity-redux is currently underway on the new generation of URu_2Si_2 crystals by two groups (Levallois et al., 2010; Lobo et al., 2010). The goal here is to perform systematic spectroscopy measurements on oriented samples down to lower frequencies and temperatures. Such experiments have probed the gradual formation of the hybridization gap which was found to start above 40 K in the KL (HFL) phase reaching a dip width of ≈ 15 meV as the temperature is reduced towards T_o . Also an anisotropic reduction of the conductivity was detected between the a and c axes due to the hybridization (Levallois et al., 2010). Hence, a reconstruction of the electronic structure already *above* T_o is suggested. The opening of the HO gap (expected to be ≈ 5 meV or 40^{-1} cm) below T_o has still not been finalized. Although clearly indicated by Lobo et al. (2010), in accordance with older measurements (Bonn et al., 1988; Degiorgi et al., 1997; Thieme et al., 1995), it had only recently been observed down to 5 K and 1.2 meV (10 cm^{-1}) in reflectivity (van der Marel, 2011). Further experiments are now in progress to systematically study the optical conductivity below the HO transition.

A new series of Shubnikov-de Haas experiments have just been completed on high-quality single crystals of URu_2Si_2 under pressure (Hassinger et al., 2010) and in high magnetic fields (Altarawneh et al., 2011). The fresh angle-dependent data of Hassinger et al. (2010), shown in Fig. 13, reveal two earlier undetected FS branches in the HO phase which has increased the observed enhanced mass to over 50 percent of that derived from specific heat. When combined with recent SdH measurements (Shishido et al., 2009), also on a high-purity single crystal, where another new, heavy branch was discovered, we now believe the FS to be definitely established. By increasing the pressure the LMAF was reached and the quantum oscillations were measured and compared to those in the HO state. There was very little change in the FS between these two phases. This is unexpected, as the HO and LMAF phases are considered to be separated by a first order phase transition (Motoyama et al., 2003). The new SdH result supports the conjecture that the lattice doubling and modified Brillouin zone of the LMAF is already present in the HO state. Hence, the suggestion arises that the HO transition breaks BCT translational symmetry. There exists fine agreement of the various angular dependent FS branches of Hassinger et al. (2010) and those predicted from DFT calculations (Oppeneer et

al., 2010); the computed FS sheets are shown in Fig. 14 and discussed further below. Thus, we know now the all-important FS of HO URu₂Si₂ and at least partially, the occurring translational symmetry breaking.

The recent high-field SdH investigation of Altarawneh et al. (2011) finds a sequence of four Fermi surface changes when the field is swept to 40 T. The field-induced modifications of the SdH oscillations are interpreted as a pocket-by-pocket magnetic polarization of the Fermi surface with increasing field, until the HO is destroyed at ~ 35 T. In addition, rotating field measurements are employed to determine the effective g -factor. Consistent with earlier dHvA experiments (Ohkuni et al., 1999) a highly angle-dependent g -factor is obtained, emphasizing the strong Ising-like anisotropy present in URu₂Si₂. A first explanation of the single-ion Ising feature was proposed in terms of the anisotropic Kondo model (Goremychkin et al., 2002). Alternatively, in an itinerant approach it originates from the strong spin-orbit coupling of U which is particularly effective for hybridized states in the presence of a reduced lattice symmetry. This interesting Ising property has not yet received the full attention it deserves.

Scanning tunneling microscopy and spectroscopy (STM/STS) have finally succeeded to detect the atomically-resolved properties of the heavy-fermion material URu₂Si₂. Two groups: Cornell (Schmidt et al., 2010) and Princeton (Aynajian et al., 2010) have mastered the art of in-situ, cold-cleaving the compound in cryogenic vacuum, thereby obtaining many tens of nanometer clean, flat surfaces for topology and spectroscopy. The issue of surface termination remains unresolved with Schmidt et al. (2010) suggesting a Si top layer. In contrast, based upon many cleaves with different surface reconstructions and their interface steps, Aynajian et al. (2010) have determined a U surface termination. Once the surface topology was established, the spectroscopy could be performed with atomic resolution to detect locally modulated structures. Figure 15 shows both the topology and the spectroscopy of the atomically resolved U surface termination. Surprisingly, as the temperature was lowered into the Kondo liquid regime, $T < 100$ K, a Fano lineshape developed in the differential conductance, dI/dV , Fig. 15c. Previously this asymmetric line shape had been associated with a single-impurity Kondo resonance due to the two interfering tunneling paths: one through the itinerant electrons, the other through the Kondo resonance, now the U-5*f* electrons. The width of the Fano spectrum which varies as a function of temperature gives an estimate of the Kondo temperature, here ≈ 120 K. The appearance of a Fano line shape in URu₂Si₂ has stimulated a mixture of theoretical descriptions (Dubi and Balatsky, 2011; Figgins and Morr, 2010; Haule and Kotliar, 2009; Maltseva et al., 2009; Wölfle et al., 2011; Yang, 2009; Yuan et al., 2011). Upon further lowering the temperature, $T < 17$ K, into the HO state a clear dip emerges within the Fano structure, i.e., the HO gap Δ_{HO} of ≈ 5 meV ap-

pears (Aynajian et al., 2010; Schmidt et al., 2010). Note the evolution of the Fano resonance below 100 K and the sharp-in-temperature appearance of the HO gap within the Fano spectrum, Fig. 15b. $\Delta_{\text{HO}}(V, T)$ is asymmetric with respect to the Fermi energy and, most importantly, its temperature dependence mimics a BCS mean-field gap opening. At the lowest temperatures, $T < 4$ K (see Fig. 15b), additional structure or modes appear within the HO gap presenting a new demand for the theory (cf. Dubi and Balatsky (2011)). By taking advantage of the atomic resolution the spatial modulations in the conductivity can be studied. Both the Fano spectrum and the HO gap are strongest between the U surface atoms. Thus it seems that the main tunneling processes or largest tunneling density of states are into hybridized electronic states that exist in-between the U-sites, i.e., involving non-localized or itinerant 5*f* electrons.

By placing Th impurities on the U-surface, Schmidt et al. (2010) were able to image quasiparticle interference patterns. When Fourier transformed, the bias voltage *vs.* the \mathbf{k} -space structure showed the splitting of a light band into two heavy bands with temperature falling below T_0 . Once again the splitting is of order of 5 meV at a $\mathbf{Q} = 0.3 a^*$, consistent with the ensemble of other measurements.

The surge of efforts in the angular resolved photoemission spectroscopy (ARPES) field is truly remarkable since eight international groups are presently involved in such challenging measurements on URu₂Si₂. Although ARPES is a most successful tool for studying the high temperature superconductors, it has been only moderately effective for the strongly correlated electron systems because of their 3D Brillouin zones, their hostile cleaving and surface properties, and the need for very low temperatures, ultra-high vacuum and extreme meV resolution. Yet early on two ARPES investigations (Denlinger et al., 2000, 2001; Ito et al., 1999) in the Kondo liquid (paramagnetic) phase attempted to compare the energy bands mapped from ARPES spectra with those of the band-structure calculations then available (Yamagami, 1998). Here the comparisons were of poor success without a direct determination of or correspondence to the U-5*f* bands near and crossing the FS.

A recent ARPES study by Santander-Syro et al. (2009) using He-lamp energies (≈ 21 eV) and a high-resolution analyzer has detected and tracked a narrow band of heavy quasi-particles that shifts from above to below the Fermi level as the temperature is reduced through the HO transition. Above E_F the narrow band appears incoherent, yet once below the Fermi level the band sharpens and disperses as a heavy-electron band that seems to be hybridized with a light-hole band at specific \mathbf{k} -values corresponding to the FS of this conduction-electron band. The measured behavior is interpreted to represent a new type of Fermi-surface instability associated with the reconstruction of portions of the FS involving heavy quasi-particles. This work suggests that KL coherence develops at the HO transition and thus not at the coherence tem-

perature $T^* \approx 70$ K. The specific data treatment applied might however play a role here. Hence, this pioneering experiment has given rise to an array of critical questions concerning the data collection method and analysis. Nonetheless, Santander-Syro et al. (2009) have demonstrated the effectiveness of ARPES in studying the HO transition in URu_2Si_2 and their work has led to the present wave of additional ARPES experiments.

Recently, Yoshida et al. (2010) performed laser ARPES using a 6 eV laser source on URu_2Si_2 and $\text{U}(\text{Ru}_{1-x}\text{Rh}_x)_2\text{Si}_2$, with $x = 0.03$. The 3% Rh substitution is sufficient to eliminate the HO. This ARPES study, which is mostly sensitive to the d -bands, reveals that a narrow, yet dispersive band suddenly *appears* below E_F when temperature is lowered to below T_o , a feature which is absent in the Rh-substituted sample. The sudden appearance of this band provides evidence for a doubling of the unit cell along the c axis in the HO, an observation that agrees with that deduced from the latest SdH measurements (Hassinger et al., 2010).

ARPES in the soft-X-ray range was also recently reported (Kawasaki et al., 2011a,b). In this energy range photoemission probes the bulk electronic structure, whereas it is particularly surface sensitive at He I and He II energies. Variation of the photonenergy reveals $5f$ -related energy bands dispersing in an energy window from -0.6 eV to E_F , which are in good agreement with band-structure calculations assuming itinerant $5f$ electrons. Moreover, these bulk sensitive ARPES measurements do not detect a narrow heavy band in the vicinity of E_F , in contrast to the He I study of Santander-Syro et al. (2009). This narrow heavy band is consequently attributed to a surface contribution.

A new technique, time and angular resolved photoemission spectroscopy (tr-ARPES) was very recently applied to study the dynamics of the HO quasiparticles on the femtosecond time scale (Dakovski et al., 2011). Within reciprocal space the probed position is first tuned to one of the Fermi surface hot spots (see below), and subsequently the femtosecond time-resolved quasiparticle dynamics at this location is probed after stimulation with a pump laser. Measurements performed below and above T_o reveal that the quasiparticle lifetime dramatically rises with one order of magnitude upon entering the HO. The formation of long-lived quasiparticles at the hot spots is identified as the principal mediator of the HO phase. Although the study proved the existence of driving quasiparticles, their precise nature could not yet be disclosed.

Contemporary theory has revisited the early band-structure calculations (Norman et al., 1988; Rozing et al., 1991) with the use of state-of-the-art electronic structure methods. Elgazzar et al. (2009) performed such calculations on URu_2Si_2 within the framework of density functional theory (DFT) within the local density approximation (LDA). While such an approach may be suspect for a strongly correlated electron system, it represents the basic starting point for more sophisticated methods. The

calculation was applied to the paramagnetic (or Kondo liquid) phase and the LMAF phase, in which there is a reasonable magnetic moment ($\sim 0.4 \mu_B$) and a conventional antiferromagnetic transition. Here the computed band structure and FS obtained from the energy dispersions showed critical regions or “hot spots” in \mathbf{k} -space where degenerate band crossings at E_F (“Dirac points”) induce FS instabilities. These accidental band degeneracies in the normal state, shown in Fig. 16 by the blue lines, causes FS gapping when symmetry breaking through antiferromagnetic ordering takes place (red lines). Thus we have the LMAF phase transition. An increase in the exchange interaction leads to a larger magnetic moment and a greater FS gap.

Applying various computational methods to treat the f electron correlations, *viz.* DFT-LDA, LDA with added strong Coulomb interaction (LDA+ U), and dynamical mean field theory (DMFT), an in-depth comparison of calculated and known experimental properties of the PM and LMAF phases was performed by Oppeneer et al. (2010). Good agreement is found throughout when the $5f$ electrons are treated as itinerant, especially regarding the ordered U-moment which is composed of opposite spin and orbital components in accord with the net measured neutron moment of $0.4 \mu_B$ (Amitsuka et al., 2007; Bourdarot et al., 2003b; Butch et al., 2010). Hence, the LMAF phase and its FS gapping is understood. Now there remains the difficulty with the HO phase since this phase is not long-range magnetically ordered, *i.e.*, there is no intrinsic HO magnetic moment. Yet we know from experiment that the HO and LMAF phases have quite similar properties, for example, the transport energy gap (Jeffries et al., 2007) and the FS (Hassinger et al., 2010; Nakashima et al., 2003). Therefore, the band-structure calculations should also apply to the HO state, provided appropriate assumptions are made for the origin of the HO. In this phase there are the long-lived, longitudinal, dynamical spin fluctuations observed in the INS resonance. Based upon this commensurate \mathbf{Q}_0 spin resonance, Elgazzar et al. (2009) proposed a novel dynamical symmetry breaking model. They argued that the antiferromagnetic spin mode causes the FS gapping and thus drives the HO transition. Here unit-cell doubling along the c axis and time-reversal symmetry breaking due to a dynamic mode were proposed for the HO in the electronic structure calculations of Elgazzar et al. (2009), leading to the FS topology shown in Fig. 14. Detailed DFT calculations of quantum oscillations have recently been performed (Oppeneer et al., 2010). The calculated extremal FS cross-sections of the theoretical FS of Fig. 14 are in good agreement with recent experimental data. There are five branches; four of these correspond to the branches detected by Hassinger et al. (2010), including the splitting of the β branch. Theory also predicts a larger ε branch (1.35 kT) that was detected by Shishido et al. (2009), but not by Hassinger et al. (2010). The commensurate spin mode drives the FS gapping and leads to the average gap magnitude as the order parameter

and the integrated intensity of the resonance (dynamical susceptibility) as a secondary order parameter. Both order parameters exhibit a BCS-like temperature dependence. A new aspect now enters the theory, namely, the time-scale of the spin resonance (Oppeneer et al., 2010). However, the central question persists: Can a dynamical mode create a phase transition?

Balatsky et al. (2009) proposed that the incommensurate spin mode at \mathbf{Q}_1 would be essential to the HO instead of the antiferromagnetic mode at \mathbf{Q}_0 . Assuming a coupling between FS sheets connected by the nesting vector \mathbf{Q}_1 , giving rise to a FS gap in the HO, they derived a form of the dynamic spin susceptibility $\chi(\mathbf{Q}_1, \omega)$ in accordance with INS measurements. Also, Balatsky et al. (2009) calculated the temperature-dependent specific heat related to the assumed FS gapping and obtained good agreement with experiment. INS studies of the commensurate spin resonance were reported recently (Bourdarot et al., 2010), similar studies at the incommensurate mode are now required to unveil their distinct contribution and relative importance.

Haule and Kotliar (2009) have presented a new theoretical approach to calculate the correlated electronic structure of URu₂Si₂ and related it to the known experimental facts. Using a combination of DFT and temperature dependent DMFT applied to a $U^{4+} - 5f^2$ localized configuration, the authors deduce a CEF scheme consisting of the $\Gamma_1^{(1)}$ and Γ_2 singlets, with a CEF splitting of ≈ 35 K. This level scheme supports a complex order parameter, consisting of a dipolar order J_z and simultaneously a hexadecapolar order, $(J_x J_y + J_y J_x)(J_x^2 - J_y^2)$. The two-singlets scheme and possible multipoles are those that were considered earlier by Nieuwenhuys (1987) and Santini and Amoretti (1994), except for the reversed order of ground and first excited state. Upon lowering the temperature the system evolves from this local $5f^2$ configuration into a multichannel Kondo state which at temperatures less than 35 K becomes “arrested” by the CEF splitting. The two phases, HO and LMAF, are treated as real, respectively, imaginary, parts of the same OP, and arise from collective CEF excitations to the excited state. Accordingly, the HO phase transition is the real part formation of the non-magnetic hexadecapole OP that breaks rotational symmetry but preserves time-reversal symmetry. Upon tuning, e.g., pressure, the imaginary part of the OP dominates and corresponds to the LMAF phase with its time-reversal symmetry breaking. Thus this complex OP treats both phases with their different symmetry breaking properties. Haule and Kotliar (2009) also calculate the one-electron spectral function which they correlate with the recent STM/STS experiments (Aynajian et al., 2010; Schmidt et al., 2010); and their results give the observed Fano resonances. The microscopic DMFT calculations furthermore determine the FS and DOS. These quantities are however disparate from those obtained in another recent DMFT calculation that started from a nearly itinerant $5f$ configuration plus a modest Coulomb interaction U (Oppeneer et al., 2010).

The FS predicted for a $5f^2$ hexadecapolar state also does not seem to be in correspondence with the recent SdH results (Hassinger et al., 2010).

In order to draw further experimental comparisons Haule and Kotliar (2010) used the above framework to develop a Landau-Ginzburg theory of the HO in URu₂Si₂. Here they consider phase modifications due to strain, pressure and magnetic field as has been studied experimentally via uniaxial stress (Yokoyama et al., 2005), thermal expansion (Motoyama et al., 2008) and neutron scattering (Aoki et al., 2009). The theory also associates the INS \mathbf{Q}_0 resonance with a pseudo-Goldstone mode which carries a fluctuating magnetic moment in the HO phase as seen in the neutron scattering. The impact of the Haule and Kotliar theory necessitates the experimental search for some evidence of the CEF levels and their splitting, which up until now has not been found. In addition with newly available x-ray techniques, e.g., x-ray Bragg diffraction (Lovesey et al., 2005) or non-resonance inelastic x-ray scattering, the observation of high-order multipolar transitions might be a future possibility (Gupta et al., 2010).

A further and different approach by Harima et al. (2010) was to present a space group analysis of the URu₂Si₂ crystal structure and thereby approach the HO transition as a change of crystal symmetry. Based upon group theoretical tabulations they find that a second-order structural transition occurs from the “mother” space group $I4/mmm$ to $P4_2/mnm$ which does not require a lattice distortion and would keep the NQR frequency at the Ru site unchanged (Saitoh et al., 2005). The analysis is performed within a localized, quadrupolar framework, adopting the Γ_5 doublet to form antiferro $J_x J_y$ quadrupoles. In order to detect the proposed charge distribution of quadrupole pairs, greatly improved resonant x-ray sensitivities are needed since up until now there is no firm experimental evidence for quadrupolar formation or its antiferro long-range order (Amitsuka et al., 2010; Walker et al., 2011).

Along similar lines Su et al. (2011) have returned to predict a CDW model using the theoretical results of the hybridization wave calculation (Dubi and Balatsky, 2011). Here the primary OP is caused by an incommensurate hybridization between light and heavy fermion bands near the Fermi level at $\mathbf{Q} = \pm 0.3a^*$. The resulting scattering between f -electrons and d -holes at $\pm \mathbf{Q}$ generates an instability forming a hybridization wave in momentum space. Experimental comparisons are drawn with the Fano resonance and HO gapping from STM/STS (Aynajian et al., 2010; Schmidt et al., 2010). The CDW is in this scenario induced as a secondary order parameter by the primary HO one. We note that during many years a vast experimental scrutiny to detect a CDW has failed. So at the present moment with many innovative efforts the search continues for the solution of the unsolved case of HO in URu₂Si₂.

Recently, Okazaki et al. (2011) performed magnetic torque measurements on URu₂Si₂ to determine the mag-

netic susceptibility in the tetragonal basal plane. The authors observed a rotational symmetry reduction, from four-fold in the paramagnetic phase to two-fold for temperatures below T_0 . They interpret this as evidence of a non-zero off-diagonal magnetic susceptibility χ_{xy} in the HO. The torque effect can be found only in one or two tiny single crystals of URu₂Si₂. Okazaki et al. (2011) propose that domain formation prevents the detection for larger crystals. According, this breaking of four-fold rotation symmetry in a tetragonal crystal is related to an electronic nematic phase, i.e., a directional electronic state in a heavy fermion metal (see, e.g., Podolsky and Demler (2005) for a discussion of spin nematic phases). The possibility of a reduction from tetragonal symmetry was earlier investigated by in-plane oriented thermal expansion measurements, but these could not detect any notable effect, $\Delta L/L < 10^{-7}$ (Kuwahara et al., 1997).

Thalmeier and Takimoto (2011) have developed a Landau free energy functional to describe the possible variety of multipolar order parameters that could be compatible with the torque measurement. Their conclusion is that an E-type, (antiferro-) two-component (O_{yz}, O_{zx}) quadrupole can best fit the two-fold torque oscillations as the HO symmetry. In addition, based upon the torque results (Okazaki et al., 2011), Pépin et al. (2011) have proposed spatially modulated spin-liquid order in the basal plane as the HO. Such order is created by a Kondo breakdown critical point. Fujimoto (2011) examines scenarios for a spin nematic state in an effective two-band model with nesting properties of the two bands as given by first-principles calculations. The spin nematic phase is proposed to be a spin-triplet electron-hole pairing state, with electron and hole particles, respectively, located in either one of the two nested bands. This leads to a d -type pairing OP that does not break time-reversal symmetry but has broken four-fold symmetry in the basal plane. Oppeneer et al. (2011) proposed that the nonzero off-diagonal susceptibility is caused by dynamical spin-orbital currents circulating around U atoms in the tetragonal planes.

These new results emphasize the question of which symmetry is spontaneously broken in the HO. The recent laser-ARPES experiments (Yoshida et al., 2010) suggest doubling of the unit cell along the c axis, in agreement with SdH data which trace a very similar FS in both the HO and LMAF (Hassinger et al., 2010). The latest torque measurements suggest a symmetry reduction in the tetragonal plane (Okazaki et al., 2011). A major question that persists is whether time-reversal symmetry is broken in the HO. Experiments have not been able to conclusively answer this question. Early on, the spurious SMAF phase obscured its clarification and even current experiments have not provided the final answer. μ SR experiments performed in the HO and LMAF phases (Amato et al., 2004) unveiled a peculiar difference: A strongly anisotropic dipolar field along the c axis in the LMAF phase, corresponding to Ising-like order, but a very weak, *isotropic* local field in the HO. This field is

not related to a spurious SMAF phase or an inhomogeneous mixing of an LMAF component, as the local field is smaller than that of $0.03 \mu_B$ ordered moments which in addition would be Ising anisotropic. The presence of the internal field could point to a time-odd phase which is however apparently distinct from the long-range dipolar ordered LMAF phase. A bothersome question is the origin of such a field. Could fluctuations of multipole states or averaging due to a spin fluctuation mode account for this?

What have we now learned about URu₂Si₂ and its HO phase? After a quarter century of intensive investigations seeking to uncover the HO, the identity of this mysterious phase remains unresolved. Yet our understanding of this intriguing heavy-fermion material and the HO has markedly increased. In 2010 finally two quantities, the FS gap and the dynamical spin susceptibility, were proven to display mean-field-like OP behavior (Aynajian et al., 2010; Bourdarot et al., 2010). These findings should thus provide a hint for where to search for the OP. Quantum oscillation measurements established a seemingly complete picture of the FS in the HO (Hassinger et al., 2010; Shishido et al., 2009). The surprisingly large entropy release at the HO transition could be attributed to a gapping of intensive long-lived spin excitations (Wiebe et al., 2007) that appear to play a critical role (Oppeneer et al., 2010). Here there clearly emerges the dominance of non-local, itinerant $5f$ electrons. In addition, at least part of the spontaneous symmetry breaking in the HO has been discovered, as there are now clear indications for unit-cell doubling along the c axis (Yoshida et al., 2010) and a first observation of four-fold rotational symmetry in the basal plane (Okazaki et al., 2011). The high-field and doping behaviors illustrate the fragility of the HO and its uniqueness among heavy-fermion materials. Some of these new observations do call for further investigation and independent confirmation, and moreover, it needs to be clarified how the various features of the HO are interconnected. We anticipate that the HO problem will continue to raise questions and challenge our understanding of how new ordered phases of matter can spontaneously emerge.

Acknowledgments

We gratefully acknowledge discussions with J. W. Allen, H. Amitsuka, P. Aynajian, A. V. Balatsky, N. Bernhoeft, M. Biasini, F. Bourdarot, W. J. L. Buyers, R. Caciuffo, P. Chandra, P. Coleman, N. J. Curro, J. D. Denlinger, A. de Visser, T. Durakiewicz, S. Elgazzar, J. Flouquet, M. Graf, H. Harima, N. Harrison, E. Hassinger, K. Haule, M. Jaime, V. Janis, J. R. Jeffries, G. Knebel, G. Kotliar, G. H. Lander, N. Magnani, M. B. Maple, D. van der Marel, Y. Matsuda, K. McEwen, Y. Ōnuki, R. Osborn, C. Pépin, C. Pfeleiderer, J. Ruzs, A. Santander-Syro, J. Schoenes, M.-T. Suzuki, P. Thalmeier, C. M. Varma, and A. Yazdani. This work has been supported

through the Swedish Research Council (VR).

Note added in proof. —After submission of this article several works on URu₂Si₂ appeared. Malone et al. (2011) measured its thermoelectric coefficients in a high magnetic field and suggest that changes of the Fermi surface topology occur deep in the HO phase at high fields. Liu et al. (2011) employed ultrafast pump-probe optical spectroscopy to monitor the response to a fs-laser pulse. The decay of the optical pumped state suggests the opening of a pseudogap below 25 K. Theoretical support for this idea was provided by Haraldsen et al. (2011) who deduced the presence of a pseudogap state from PCS measurements. Toth and Kotliar (2011) proposed a localized hexadecapolar Kondo effect in diluted URu₂Si₂. Further, the most recent experimental studies on URu₂Si₂ are by Niklowitz et al. (2011), who performed quasielastic scattering from the \mathbf{Q}_0 and \mathbf{Q}_1 resonances, Bourdarot et al. (2011), who performed neutron scattering under uniaxial stress, and Nagel et al. (2011) who made a Fermi liquid analysis of the optical conductivity.

References

- Altarawneh, M. M., N. Harrison, S. E. Sebastian, L. Balicas, P. H. Tobash, J. D. Thompson, F. Ronning, and E. D. Bauer, 2011, Phys. Rev. Lett. **106**, 146403.
- Amato, A., M. J. Graf, A. de Visser, H. Amitsuka, D. Andreica, and A. Schenck, 2004, J. Phys.: Condens. Matter **16**, S4403.
- Amitsuka, H., K. Hyomi, T. Nishioka, Y. Miyako, and T. Suzuki, 1988, J. Magn. Magn. Mater. **76**, 168.
- Amitsuka, H., and T. Sakakibara, 1994, J. Phys. Soc. Jpn. **63**, 736.
- Amitsuka, H., M. Sato, N. Metoki, M. Yokoyama, K. Kuwahara, T. Sakakibara, H. Morimoto, S. Kawarazaki, Y. Miyako, and J. A. Mydosh, 1999, Phys. Rev. Lett. **83**, 5114.
- Amitsuka, H., K. Matsuda, I. Kawasaki, K. Tenya, M. Yokoyama, C. Sekine, N. Tateiwa, T. C. Kobayashi, S. Kawarazaki, and H. Yoshizawa, 2007, J. Magn. Magn. Mater. **310**, 214.
- Amitsuka, H., T. Inami, M. Yokoyama, S. Takayama, Y. Ikeda, I. Kawasaki, Y. Homma, H. Hidaka, and T. Yanagisawa, 2010, J. Phys.: Conf. Series **200**, 012007.
- Aoki, D., F. Bourdarot, E. Hassinger, G. Knebel, A. Miyake, S. Raymond, V. Taufour, and J. Flouquet, 2009, J. Phys. Soc. Jpn. **78**, 053701.
- Aynajian, P., E. H. da Silva Neto, C. V. Parker, Y.-K. Huang, A. Pasupathy, J. A. Mydosh and A. Yazdani, 2010, Proc. Natl. Acad. USA **107**, 10383.
- Baek, S.-H., M. J. Graf, A. V. Balatsky, E. D. Bauer, J. C. Cooley, J. L. Smith, and N. J. Curro, 2010, Phys. Rev. B **81**, 132404.
- Balatsky, A. V., A. Chantis, H. P. Dahal, D. Parker, and J. X. Zhu, 2009, Phys. Rev. B **79**, 214413.
- Barzykin, V., and L. P. Gor'kov, 1993, Phys. Rev. Lett. **70**, 2479.
- Barzykin, V., and L. P. Gor'kov, 1995, Phys. Rev. Lett. **74**, 4301.
- Behnia, K., R. Bel, Y. Kasahara, H. Jin, H. Aubin, K. Izawa, Y. Matsuda, J. Flouquet, Y. Haga, Y. Ōnuki, and P. Lejay, 2005, Phys. Rev. Lett. **94**, 156405.
- Bel, R., H. Jin, K. Behnia, J. Flouquet, and P. Lejay, 2004, Phys. Rev. B **70**, 22050(R).
- Bernal, O. O., C. Rodrigues, A. Martinez, H. G. Lukefahr, D. E. MacLaughlin, A. A. Menovsky, and J. A. Mydosh, 2001, Phys. Rev. Lett. **87**, 196402.
- Bernal, O. O., M. E. Moroz, K. Ishida, H. Murakawa, A. P. Reyes, P. L. Kuhns, D. E. MacLaughlin, J. A. Mydosh, and T. J. Gortenmulder, 2006, Physica B **378-380**, 574.
- Biasini, M., J. Ruzs, and A. P. Mills, 2009, Phys. Rev. B **79**, 085115.
- Bonn, D. A., J. D. Garrett, and T. Timusk, 1988, Phys. Rev. Lett. **61**, 1305.
- Bourdarot, F., B. Fåk, K. Habicht, and K. Prokes, 2003a, Phys. Rev. Lett. **90**, 067203.
- Bourdarot, F., B. Fåk, V. P. Minnev, M. E. Zhitomirsky, N. Kernavanois, S. Raymond, P. Burlet, F. Lapiere, P. Lejay, and J. Flouquet, 2003b, ArXiv:cond-mat/0312206v1.
- Bourdarot, F., A. Bombardi, P. Burlet, M. Enderle, J. Flouquet, P. Lejay, N. Kernavanois, V. P. Mineev, L. Paolasini, M. E. Zhitomirsky, and B. Fåk, 2005, Physica B **359-361**, 986.
- Bourdarot, F., E. Hassinger, S. Raymond, D. Aoki, V. Taufour, L.-P. Regnault, and J. Flouquet, 2010, J. Phys. Soc. Jpn. **79**, 064719.
- Bourdarot, F., et al., 2011, arXiv:cond-mat/1110.5157.
- Broholm C., J. K. Kjems, W. J. L. Buyers, P. Matthews, T. T. M. Palstra, A. A. Menovsky, and J. A. Mydosh, 1987, Phys. Rev. Lett. **58**, 1467.
- Broholm C., H. Lin, P. T. Matthews, T. E. Mason, W. J. L. Buyers, M. F. Collins, A. A. Menovsky, J. A. Mydosh, and J. K. Kjems, 1991, Phys. Rev. B **43**, 12809.
- Butch, N. P., and M. B. Maple, 2009, Phys. Rev. Lett. **103**, 076404.
- Butch, N. P., J. R. Jeffries, S. Chi, J. Batista Leão, J. W. Lynn, and M. B. Maple, 2010, Phys. Rev. B **82**, 060408(R).
- Buyers, W. J. L., 1996, Physica B **223-224**, 9.
- Chandra, P., P. Coleman, J. A. Mydosh, and V. Tripathi, 2002, Nature (London), **417**, 831.
- Coleman, P., and A. J. Schofield, 2005, Nature (London) **433**, 226.
- Cox, D. L., 1987, Phys. Rev. Lett. **59**, 1240.
- Cricchio, F., F. Bultmark, O. Grånäs, and L. Nordström, 2009, Phys. Rev. Lett. **103**, 107202.
- Dakovski, G. L., Y. Li, S. M. Gilbertson, G. Rodriguez, A. V. Balatsky, J.-X. Zhu, K. Gofryk, E. D. Bauer, P. H. Tobash, A. Taylor, J. L. Sarrao, P. M. Oppeneer, P. S. Riseborough, J. A. Mydosh, and T. Durakiewicz, 2011, Phys. Rev. B **84**, 161103(R).
- Dalla Torre, E. G., E. Berg, and E. Altman, 2006, Phys. Rev. Lett. **97**, 26041.
- de Boer, F. R., J. J. M. Franse, E. Louis, A. A. Menovsky, J. A. Mydosh, T. T. M. Palstra, U. Rauchschwalbe, W. Schlabitz, F. Steglich, and A. de Visser, 1986, Physica B **138**, 1.
- Degiorgi, L., St. Thieme, H. R. Ott, M. Dressel, G. Grüner, Y. Dalichaouch, M. B. Maple, Z. Fisk, C. Geibel, and F. Steglich, 1997, Z. Phys. B **102**, 367.
- Denlinger, J. D., G.-H. Gweon, J. W. Allen, C. G. Olson, Y. Dalichaouch, B.-W. Lee, M. B. Maple, Z. Fisk, P. C. Canfield, and P. E. Armstrong, 2000, Physica B **281-282**, 716.
- Denlinger, J. D., G.-H. Gweon, J. W. Allen, C. G. Olson, M. B. Maple, J. L. Sarrao, P. E. Armstrong, Z. Fisk, and H. Yamagami, 2001, J. Electron Spectrosc. Relat. Phenom.

- 117-118, 347.
- de Visser, A., F. E. Kayzel, A. A. Menovsky, J. J. M. Franse, J. van den Berg, and G. J. Nieuwenhuys, 1986, Phys. Rev. B **34**, 8168.
- Dubi, Y., and A. V. Balatsky, 2011, Phys. Rev. Lett. **106**, 086401.
- Elgazzar, S., J. Ruzs, M. Amft, P. M. Oppeneer, and J. A. Mydosh, 2009, Nature Mater. **8**, 337.
- Escudero, R., F. Morales, and P. Lejay, 1994, Phys. Rev. B **49**, 15271.
- Fazekas, P., A. Kiss, and K. Radnóczy, 2005, Prog. Theor. Phys. Suppl. **160**, 114.
- Figgins, J., and D. Morr, 2010, Phys. Rev. Lett. **104**, 187202.
- Fisher, R. A., S. Kim, Y. Wu, N. E. Phillips, M. W. McElfresh, M. S. Torikachvili, and M. B. Maple, 1990, Physica B **163**, 419.
- Fujimoto, S., 2011, Phys. Rev. Lett. **106**, 196407.
- Goremeychkin, E. A., R. Osborn, B. D. Rainford, T. A. Costi, A. P. Murani, C. A. Scott, and P. J. C. King, 2002, Phys. Rev. Lett. **89**, 147201.
- Gor'kov, L. P., 1991, Europhys. Lett. **16**, 301.
- Gor'kov, L. P., and A. Sokol, 1992, Phys. Rev. Lett. **69**, 2586.
- Gupta, S. S., J. A. Bradely, M. W. Haverkort, G. T. Seidler, A. Tanaka, and G. A. Sawatzky, 2010, ArXiv:cond-mat/1001.5293v1.
- Hanzawa, K., 2007, J. Phys.: Condens. Matter **19**, 072202.
- Hanzawa, K., and N. Watanabe, 2005, J. Phys.: Condens. Matter **17**, L419.
- Haraldsen, J. T., Y. Dubi, N. J. Curro, and A. V. Balatsky, 2011, ArXiv:cond-mat/1104.2931.
- Harima, H., K. Miyake, and J. Flouquet, 2010, J. Phys. Soc. Jpn. **79**, 033705.
- Harrison, N., M. Jaime, and J. A. Mydosh, 2003, Phys. Rev. Lett. **90**, 096402.
- Hasan, M. Z., and C. L. Kane, 2010, Rev. Mod. Phys. **82**, 3045.
- Hasselbach, K., J. R. Kirtley, and P. Lejay, 1992, Phys. Rev. B **46**, 5826.
- Hassinger, E., J. Derr, J. Levallois, D. Aoki, K. Behnia, F. Bourdarot, G. Knebel, C. Proust, and J. Flouquet, 2008a, J. Phys. Soc. Jpn. **77**, Suppl. A, 172.
- Hassinger, E., G. Knebel, K. Izawa, P. Lejay, B. Salce, and J. Flouquet, 2008b, Phys. Rev. B **77**, 115117.
- Hassinger, E., G. Knebel, T. D. Matsuda, D. Aoki, V. Taufour, and J. Flouquet, 2010, Phys. Rev. Lett. **105**, 216409.
- Haule, K., and G. Kotliar, 2009, Nature Phys. **5**, 796.
- Haule, K., and G. Kotliar, 2010, Europhys. Lett. **89**, 57006.
- He, R.-H., M. Hashimoto, H. Karapetyan, J. D. Koralek, J. P. Hinton, J. P. Testaud, V. Nathan, Y. Yoshida, H. Yao, K. Tanaka, W. Meevasana, R. G. Moore, D. H. Lu, S.-K. Mo, M. Ishikado, H. Eisaki, Z. Hussain, T. P. Devereaux, S. A. Kivelson, J. Orenstein, A. Kapitulnik, and Z.-X. Shen, 2011, Science **331**, 1579.
- Hill, J. A., 1970, in *Plutonium and Other Actinides*, edited by N. W. Miner (The Metallurgical Society of the AIME, New York).
- Ikeda, H., and Y. Ohashi, 1998, Phys. Rev. Lett. **81**, 3723.
- Isaacs, E. D., D. B. McWhan, R. N. Kleiman, D. J. Bishop, G. E. Ice, P. Zschack, B. D. Gaulin, T. E. Mason, J. D. Garrett, and W. J. L. Buyers, 1990, Phys. Rev. Lett. **65**, 3185.
- Ito, T., H. Kumigashira, T. Takahashi, Y. Haga, E. Yamamoto, T. Honma, H. Ohkuni, and Y. Ōnuki, 1999, Phys. Rev. B **60**, 13390.
- Janik, J. A., 2008, unpublished, Ph.D. Thesis, Florida State University.
- Janik, J. A., H. D. Zhou, Y.-J. Jo, L. Balicas, G. J. MacDougall, G. M. Luke, J. D. Garrett, K. J. McClellan, E. D. Bauer, J. L. Sarrao, Y. Qiu, J. R. D. Copley, Z. Yamani, W. J. L. Buyers, and C. R. Wiebe, 2009, J. Phys.: Condens. Matter **21**, 192202.
- Jaime, M., 2007, unpublished.
- Jaime, M., K. H. Kim, G. Jorge, S. McCall, and J. A. Mydosh, 2002, Phys. Rev. Lett. **89**, 287201.
- Jeffries, J. R., N. P. Butch, B. T. Yukich, and M. B. Maple, 2007, Phys. Rev. Lett. **99**, 217207.
- Jeffries, J. R., N. P. Butch, B. T. Yukich, and M. B. Maple, 2008, J. Phys.: Condens. Matter **20**, 095225.
- Jeffries, J.R., K.T. Moore, N. P. Butch, and M. B. Maple, 2010, Phys. Rev. B **82**, 033103.
- Jo, Y. J., L. Balicas, C. Capan, K. Behnia, P. Lejay, J. Flouquet, J. A. Mydosh, and P. Schlottmann, 2007, Phys. Rev. Lett. **98**, 166404.
- Kasahara, Y., T. Iwasawa, H. Shishido, T. Shibauchi, K. Behnia, Y. Haga, T. D. Matsuda, Y. Ōnuki, M. Sigrist, and Y. Matsuda, 2007, Phys. Rev. Lett. **99**, 116402.
- Kasahara, Y., H. Shishido, T. Shibauchi, Y. Haga, T. D. Matsuda, Y. Ōnuki, and Y. Matsuda, 2009, New J. Phys. **11**, 055061.
- Kasuya, T., 1997, J. Phys. Soc. Jpn. **66**, 3348.
- Kawasaki, I., S.-i. Fujimori, Y. Takeda, T. Okane, A. Yasui, Y. Saitoh, H. Yamagami, Y. Haga, E. Yamamoto, and Y. Ōnuki, 2011a, J. Phys.: Conf. Ser. **273**, 012039.
- Kawasaki, I., S.-i. Fujimori, Y. Takeda, T. Okane, A. Yasui, Y. Saitoh, H. Yamagami, Y. Haga, E. Yamamoto, and Y. Ōnuki, 2011b, Phys. Rev. B **83**, 235121.
- Kim, J. S., D. Hall, P. Kumar, and G. R. Stewart, 2003a, Phys. Rev. B **67**, 014404.
- Kim, K. H., N. Harrison, M. Jaime, G. S. Boebinger, and J. A. Mydosh, 2003b, Phys. Rev. Lett. **91**, 256401.
- Kim, K. H., N. Harrison, H. Amitsuka, G. A. Jorge, M. Jaime, and J. A. Mydosh, 2004, Phys. Rev. Lett. **93**, 206402.
- Kiss, A., and P. Fazekas, 2005, Phys. Rev. B **71**, 054415.
- Kohori, Y., K. Matsuda, and T. Kohara, 1996, J. Phys. Soc. Jpn. **65**, 1083.
- Kotetes, P., and G. Varelogiannis, 2010a, Phys. Rev. Lett. **104**, 106404.
- Kotetes, P., A. Aperis, and G. Varelogiannis, 2010b, ArXiv:cond-mat/1002.2719.
- Kuramoto, Y., H., Kusunose, and A. Kiss, 2009, J. Phys. Soc. Jpn. **78**, 072001.
- Kusunose, H., and H. Harima, 2011, J. Phys. Soc. Jpn. **80**, 084702.
- Kuwahara, K., H. Amitsuka, T. Sakakibara, O. Suzuki, S. Nakamura, T. Goto, M. Mihalik, A. A. Menovsky, A. de Visser, and J. J. M. Franse, 1997, J. Phys. Soc. Jpn. **66**, 3251.
- Kuwahara, K., M. Koghi, K. Iwasa, M. Nishi, K. Nakajima, M. Yokoyama, and H. Amitsuka, 2006, Physica B **378**–**380**, 581.
- Levallois, J., K. Behnia, J. Flouquet, P. Lejay, and C. Proust, 2009, Europhys. Lett. **85**, 27003.
- Levallois, J., F. Lévy-Bertrand, M. K. Tran, J. A. Mydosh, Y.-K. Huang, and D. van der Marel, 2010, ArXiv:cond-mat/1007.538.
- Liu, M. K., et al., 2011, Phys. Rev. B **84**, 161101(R).
- Lobo, R., C. C. Homes, and P. Lejay, 2010, private communication.

- Lovesey, S. W., E. Balcar, K. S. Knight, and J. Fernández Rodríguez, 2005, *Phys. Reports* **411**, 233.
- Luke, G. M., A. Keren, L. P. Le, Y. J. Uemura, W. D. Wu, D. Bonn, L. Taillefer, J. D. Garrett, and Y. Ōnuki, 1994, *Hyperfine Inter.* **85**, 397.
- MacLaughlin, D. E., D. W. Cooke, R. H. Heffner, R. L. Hutson, M. W. McElfresh, M. E. Schillaci, H. D. Rempp, J. L. Smith, J. O. Willis, E. Zirngiebl, C. Boekema, R. L. Lichti, and J. Oostens, 1988, *Phys. Rev. B* **37**, 3153.
- Malone, L., et al., 2011, *Phys. Rev. B* **83**, 245117.
- Maltseva, M., M. Dzero, and P. Coleman, 2009, *Phys. Rev. Lett.* **103**, 206402.
- Manna, R. S., M. de Souza, A. Brühl, J. A. Schlueter, and M. Lang, 2010, *Phys. Rev. Lett.* **104**, 016403.
- Maple, M. B., J. W. Chen, Y. Dalichaouch, T. Kohara, C. Rossel, M. S. Torikachvili, M. W. McElfresh, and J. D. Thompson, 1986, *Phys. Rev. Lett.* **56**, 185.
- Marumoto, K., T. Takeuchi, and Y. Miyako, 1996, *Phys. Rev. B* **54**, 12194.
- Mason, T. E., B. D. Gaulin, J. D. Garrett, Z. Tun, W. J. L. Buyers, and E. D. Isaacs, 1990, *Phys. Rev. Lett.* **65**, 3189.
- Mason, T. E., W. J. L. Buyers, T. Petersen, A. A. Menovsky, and J. D. Garrett, 1995, *J. Phys.: Condens. Matter* **7**, 5089.
- Matsuda, K., Y. Kohori, and T. Kohara, 1996, *J. Phys. Soc. Jpn.* **65**, 679.
- Matsuda, K., Y. Kohori, T. Kohara, E.K. Kuwahara, and H. Amitsuka, 2001, *Phys. Rev. Lett.* **87**, 087203.
- Matsuda, K., Y. Kohori, T. Kohara, H. Amitsuka, K. Kuwahara, and T. Matsumoto, 2003, *J. Phys.: Condens. Matter* **15**, 2363.
- Matsuda, T. D., D. Aoki, S. Ikeda, E. Yamamoto, Y. Haga, H. Ohkuni, R. Settai, and Y. Ōnuki, 2008, *J. Phys. Soc. Jpn.* **77**, Suppl. A, 362.
- Matsuda, T. D., E. Hassinger, D. Aoki, V. Taufour, G. Knebel, N. Tateiwa, E. Yamamoto, Y. Haga, Y. Ōnuki, Z. Fisk, and J. Flouquet, 2011, *J. Phys. Soc. Jpn.* **80**, 114710.
- McElfresh, M. W., J. D. Thompson, J. O. Willis, M. B. Maple, T. Kohara, and M. S. Torikachvili, 1987, *Phys. Rev. B* **35**, 43.
- Mihalik, M., A. Kolomiets, J.-C. Griveau, A. V. Andreev, and V. Sechovský, 2006, *High Press. Res.* **26**, 479.
- Mineev, V. P., and M. E. Zhitomirsky, 2005, *Phys. Rev. B* **72**, 014432.
- Moore, K. T., and G. van der Laan, 2009, *Rev. Mod. Phys.* **81**, 235.
- Morales, F., and R. Escudero, 2009, *J. Low Temp. Phys.* **154**, 68.
- Motoyama, G., T. Nishioka, and N. K. Sato, 2003, *Phys. Rev. Lett.* **90**, 166402.
- Motoyama, G., N. Yokoyama, A. Sumiyama, and Y. Oda, 2008, *J. Phys. Soc. Jpn.* **77**, 123710.
- Nagel, U., et al., 2011, arXiv:cond-mat/1107.5574.
- Nakashima, M., H. Ohkuni, Y. Inada, R. Setti, Y. Haga, E. Yamamoto, and Y. Ōnuki, 2003, *J. Phys.: Condens. Matter* **15**, S2011.
- Nieuwenhuys, G. J., 1987, *Phys. Rev. B* **35**, 5260.
- Niklowitz, P. G., C. Pfleiderer, T. Keller, M. Vojta, Y.-K. Huang and J. A. Mydosh, 2010, *Phys. Rev. Lett.* **104**, 106406.
- Niklowitz, P. G., et al., 2011, arXiv:cond-mat/1110.5599.
- Norman, M. R., T. Oguchi, and A. J. Freeman, 1988, *Phys. Rev.* **38**, 11193.
- Oh, Y. S., K.-H. Kim, P. A. Sharma, N. Harrison, H. Amitsuka, and J. A. Mydosh, 2007, *Phys. Rev. Lett.* **98**, 016401.
- Ohkawa, F., and H. Shimizu, 1999, *J. Phys.: Condens. Matter* **11**, L519.
- Ohkuni, H., Y. Tokiwa, K. Sakurai, R. Settai, T. Haga, E. Yamamoto, Y. Ōnuki, H. Yamagami, S. Takahashi, and T. Yanagisawa, 1999, *Phil. Mag. B* **79**, 1045.
- Okazaki, R., Y. Kasahara, H. Shishido, M. Konczykowski, K. Behnia, Y. Haga, T. D. Matsuda, Y. Onuki, T. Shibauchi, and Y. Matsuda, 2008, *Phys. Rev. Lett.* **100**, 037004.
- Okazaki, R., T. Shibauchi, H. J. Shi, Y. Haga, T. D. Matsuda, E. Yamamoto, Y. Onuki, H. Ikeda, and Y. Matsuda, 2011, *Science* **331**, 439.
- Okuno, Y., and K. Miyake, 1998, *J. Phys. Soc. Jpn.* **67**, 2469.
- Oppeneer, P. M., J. Rusz, S. Elgazzar, M.-T. Suzuki, T. Durakiewicz, and J. A. Mydosh, 2010, *Phys. Rev. B* **82**, 205103.
- Oppeneer, P. M., S. Elgazzar, J. Rusz, Q. Feng, T. Durakiewicz, and J. A. Mydosh, 2011, arXiv:cond-mat/1110.0981.
- Ott, H. R., H. Rudigier, Z. Fisk, and J. L. Smith, 1983, *Phys. Rev. Lett.* **50**, 1595.
- Paixão, J. A., C. Detlefs, M. J. Longfield, R. Caciuffo, P. Santini, N. Bernhoeft, J. Rebizant, and G. H. Lander, 2002, *Phys. Rev. Lett.* **89**, 187202.
- Palstra, T. T. M., A. A. Menovsky, J. van den Berg, A. J. Dirkmaat, P. H. Kes, G. J. Nieuwenhuys, and J. A. Mydosh, 1985, *Phys. Rev. Lett.* **55**, 2727.
- Palstra, T. T. M., A. A. Menovsky, and J. A. Mydosh, 1986, *Phys. Rev. B* **33**, 6527(R).
- Pépin, C., M. R. Norman, S. Burdin, and A. Ferraz, 2011, *Phys. Rev. Lett.* **106**, 106601.
- Pezzoli, M. E., M. J. Graf, K. Haule, G. Kotliar, and A. V. Balatsky, 2011, *Phys. Rev. B* **83**, 235106.
- Pfleiderer, C., 2009, *Rev. Mod. Phys.* **81**, 1551.
- Pfleiderer, C., J. A. Mydosh, and M. Vojta, 2006, *Phys. Rev. B* **74**, 104412.
- Podolsky, D., and E. Demler, 2005, *New J. Phys.* **7**, 59.
- Ramirez, A. P., P. Coleman, P. Chandra, E. Brück, A. A. Menovsky, Z. Fisk, and E. Bucher, 1992, *Phys. Rev. Lett.* **68**, 2680.
- Rodrigo, J. G., F. Guinea, S. Vierira, and F. G. Aliev, 1997, *Phys. Rev. B* **55**, 14318.
- Roizing, G. J., P. E. Mijnenrens, and D. D. Koelling, 1991, *Phys. Rev. B* **43**, 9515.
- Saitoh, S., S. Takagi, M. Yokoyama, and H. Amitsuka, 2005, *J. Phys. Soc. Jpn.* **74**, 2209.
- Santander-Syro, A. F., M. Klein, F. L. Boariu, A. Nuber, P. Lejay, and F. Reinert, 2009, *Nature Phys.* **5**, 637.
- Santini, P., 1998, *Phys. Rev. B* **57**, 5191.
- Santini, P., and G. Amoretti, 1994, *Phys. Rev. Lett.* **73**, 1027.
- Santini, P., and G. Amoretti, 1995, *Phys. Rev. Lett.* **74**, 4098.
- Santini, P., R. Lémanski, and P. Erdős, 1999, *Adv. Phys.* **48**, 537.
- Santini, P., S. Carretta, N. Magnani, G. Amoretti, and R. Caciuffo, 2006, *Phys. Rev. Lett.* **97**, 207203.
- Santini, P., S. Carretta, G. Amoretti, R. Caciuffo, N. Magnani, and G. H. Lander, 2009, *Rev. Mod. Phys.* **81**, 807.
- Sato, H., 2008, *J. Phys. Soc. Jpn.* **77**, Suppl. A, 1.
- Schlabitz, W., J. Baumann, R. Pollit, U. Rauchschwalbe, H. M. Mayer, U. Ahlheim, and C. D. Bredl, 1986, *Z. Phys. B* **62**, 171.
- Schmidt, A. R., M. H. Hamidian, P. Wahl, F. Meier, A. V. Balatsky, J. D. Garrett, T. J. Williams, G. M. Luke, and J. C. Davis, 2010, *Nature (London)* **465**, 570.
- Schoenes, J., C. Schönenberger, J. J. M. Franse, and A. A.

- Menovsky, 1987, Phys. Rev. B **35**, 5375.
- Sechovský, V., and L. Havela, 1998, in *Handbook of Magnetic Materials*, edited by K. H. J. Buschow, Vol. 11 (Elsevier Science, Amsterdam, The Netherlands), pp. 1-289.
- Shah, N., P. Chandra, P. Coleman, and J. A. Mydosh, 2000, Phys. Rev. B **61**, 564.
- Sharma, P. A., N. Harrison, M. Jaime, Y. S. Oh, K. H. Kim, C. D. Batista, H. Amitsuka, and J. A. Mydosh, 2006, Phys. Rev. Lett. **97**, 156401.
- Shishido, H., K. Hashimoto, T. Shibauchi, T. Sasaki, H. Oizumi, N. Kobayashi, T. Takamasu, K. Takehana, Y. Imanaka, T.D. Matsuda, Y. Haga, Y. Onuli, and Y. Matsuda, 2009, Phys. Rev. Lett. **102**, 156403.
- Sikkema, A. E., W. J. L. Buyers, I. Affleck, and J. Gan, 1996, Phys. Rev. B **54**, 9322.
- Silhanek, A. V., N. Harrison, C. D. Batista, M. Jaime, A. Lacerda, H. Amitsuka, and J. A. Mydosh, 2005, Phys. Rev. Lett. **95**, 026403.
- Silhanek, A. V., M. Jaime, N. Harrison, V. R. Fanelli C. D. Batista, H. Amitsuka, S. Nakatsuji, L. Balicas, K. H. Kim, Z. Fisk, J. L. Sarrao, L. Civale, and J. A. Mydosh, 2006a, Phys. Rev. Lett. **96**, 136403.
- Silhanek, A. V., N. Harrison, C. D. Batista, M. Jaime, A. Lacerda, H. Amitsuka, and J. A. Mydosh, 2006b, Physica B (Amsterdam) **378-380**, 373.
- Smith, J. L., and E. A. Kmetko, 1983, J. Less-Comm. Metals **90**, 83.
- Stewart, G. R., 2001, Rev. Mod. Phys. **73**, 797.
- Stewart, G. R., 2006, Rev. Mod. Phys. **78**, 743.
- Stewart, G. R., Z. Fisk, J. O. Willis, and J. L. Smith, 1984, Phys. Rev. Lett. **52**, 679.
- Su, J.-J., Y. Dubi, P. Wölfe, and A. V. Balatsky, 2011, J. Phys. Condens. Matter **23**, 094214.
- Suzuki, M.-T., N. Magnani, and P. M. Oppeneer, 2010, Phys. Rev. B **82**, 241103(R).
- Sugiyama, K., H. Fuke, K. Kindo, K. Shimohata, A. A. Menovsky, J. A. Mydosh, and M. Date, 1990, J. Phys. Soc. Jpn. **59**, 3331.
- Takagi, S., S. Ishihara, S. Saitoh, H.-I. Sasaki, H. Tanida, M. Yokoyama, and H. Amitsuka, 2007, J. Phys. Soc. Jpn. **76**, 033708.
- Thalmeier, P., and T. Takimoto, 2011, Phys. Rev. B **83**, 165110.
- Thieme, St., P. Steiner, L. Degiorgi, P. Wachter, Y. Dalichaouch, and M. B. Maple, 1995, Europhys. Lett. **32**, 367.
- Tokunaga, Y., Y. Homma, S. Kambe, D. Aoki, H. Sakai, E. Yamamoto, A. Nakamura, Y. Shiokawa, R. E. Walstedt, and H. Yasuoka, 2005, Phys. Rev. Lett. **94**, 137209.
- Toth, A., P. Chandra, P. Coleman, G. Kotliar, and H. Amitsuka, 2010, Phys. Rev. B **82**, 23516.
- Toth, A., and G. Kotliar, 2011, arXiv:cond-mat/1106.5768.
- Tripathi, V., P. Chandra, and P. Coleman, 2005, J. Phys.: Condens. Matter, **17**, 5285.
- Valla, T., A. V. Fedorov, J. Lee, J. C. Davis, and G. D. Gu, 2006, Science **314**, 1914.
- van der Marel, D., 2011, private communication.
- Varma, C. M., and L. Zhu, 2006, Phys. Rev. Lett. **96**, 036405.
- Villaume, A., F. Bourdarot, E. Hassinger, S. Raymond, V. Taufour, D. Aoki, and J. Flouquet, 2008, Phys. Rev. B **78**, 012504.
- Walker, H. C., K. A. McEwen, D. F. McMorrow, S. B. Wilkins, F. Wastin, E. Colineau, and D. Fort, 2006, Phys. Rev. Lett. **97**, 137203.
- Walker, H. C., R. Caciuffo, D. Aoki, F. Bourdarot, G. H. Lander, and J. Flouquet, 2011, Phys. Rev. B **83**, 193102.
- Walker, M. B., W. J. L. Buyers, Z. Tun, W. Que, A. A. Menovsky, and J. D. Garrett, 1993, Phys. Rev. Lett. **71**, 2630.
- Walker, M. B., and W. J. L. Buyers, 1995, Phys. Rev. Lett. **74**, 4097.
- Walter, U., C.-K. Loong, M. Loewenhaupt, and W. Schlabitz, 1986, Phys. Rev. B **33**, 7875(R).
- Wiebe, C. R., G. M. Luke, Z. Yamani, A. A. Menovsky, and W. J. L. Buyers, 2004, Phys. Rev. B **69**, 132418.
- Wiebe, C. R., J. A. Janik, G. J. MacDougall, G. M. Luke, J. D. Garrett, H. D. Zhou, Y.-J. Jo, L. Balicas, Y. Qiu, J. R. D. Copley, Z. Yamani, and W. J. L. Buyers, 2007, Nature Phys. **3**, 96.
- Wolf, B., W. Sixl, R. Graf, D. Finsterbusch, G. Bruls, B. Lüthi, E. A. Knetsch, A. A. Menovsky, and J. A. Mydosh, 1994, J. Low Temp. Phys. **94**, 307.
- Wölfe, P., Y. Dubi, and A. V. Balatsky, 2010, Phys. Rev. Lett. **105**, 246401.
- Xu, G., C. Broholm, Y.-A. Soh, G. Aeppli, J. F. DiTusa, Y. Chen, M. Kenzelmann, C. D. Frost, T. Ito, K. Oka, and H. Takagi, 2007, Science, **317**, 1049.
- Yamagami, H., 1998, J. Phys. Soc. Jpn. **67**, 3176.
- Yamagami, H., and N. Hamada, 2000, Physica B **284-288**, 1295.
- Yang, Y.-F., Z. Fisk, H.-O. Lee, J. D. Thompson, and D. Pines, 2008, Nature (London) **454**, 611.
- Yang, Y.-F., 2009, Phys. Rev. B **79**, 241107(R).
- Yano, K., T. Sakakibara, T. Tayama, M. Yokoyama, H. Amitsuka, Y. Homma, P. Miranović, M. Ichioka, Y. Tsutsumi, and K. Machida, 2008, Phys. Rev. Lett. **100**, 017004.
- Yokoyama, M., H. Amitsuka, K. Kuwahara, K. Tenya, and T. Sakakibara, 2002, J. Phys. Soc. Jpn. **71**, 3037.
- Yokoyama, M., H. Amitsuka, K. Kenya, K. Watanabe, S. Kawarazaki, H. Yoshizawa, and J. A. Mydosh, 2005, Phys. Rev. B **72**, 214419.
- Yoshida, R., Y. Nakamura, M. Fukui, Y. Haga, E. Yamamoto, Y. Ōnuki, M. Okawa, S. Shin, M. Hirai, Y. Muraoka, and T. Yokoya, 2010, Phys. Rev. B **82**, 205108.
- Yuan, T., J. Figgins, and D. K. Morr, 2011, ArXiv:cond-mat/1101.2636v1.

Figures

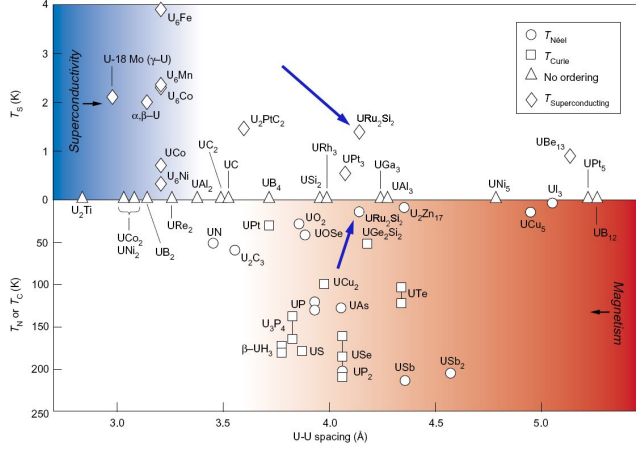


FIG. 1 (Color online) The Hill plot for various uranium-based intermetallic compounds. The bottom arrow indicates the hidden order transition temperature, T_o , of URu_2Si_2 while the top one its superconducting transition temperature, T_c . After Janik, unpublished (2008) and Moore and van der Laan (2009).

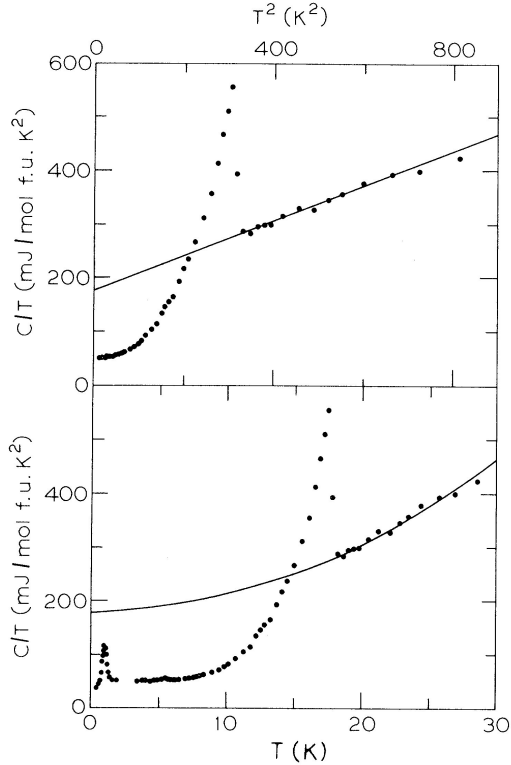


FIG. 2 Specific heat as function of temperature for URu_2Si_2 . Top: C/T vs. T^2 ; bottom: C/T vs. T with the superconducting transition also shown. Note the large extrapolated specific-heat coefficient, γ , of 180 mJ/moleK^2 . From Palstra et al. (1985).

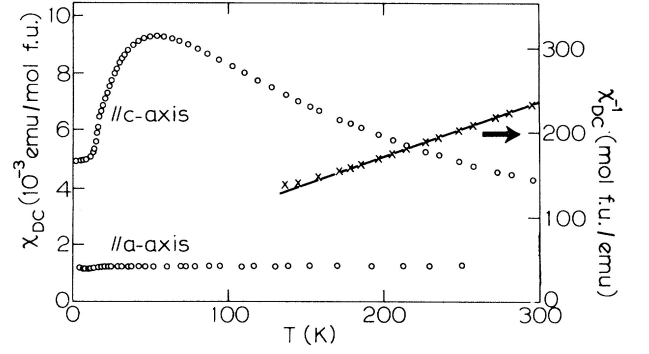
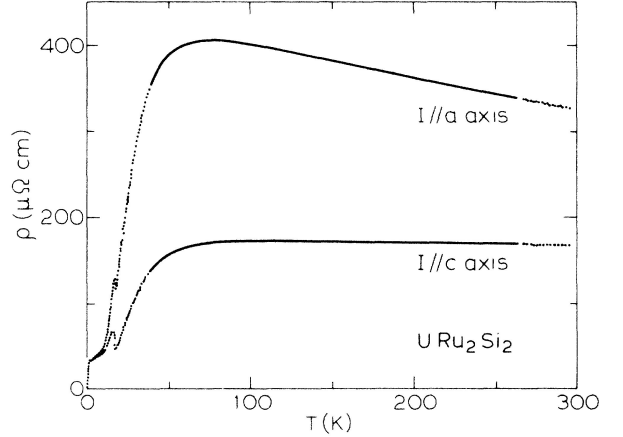
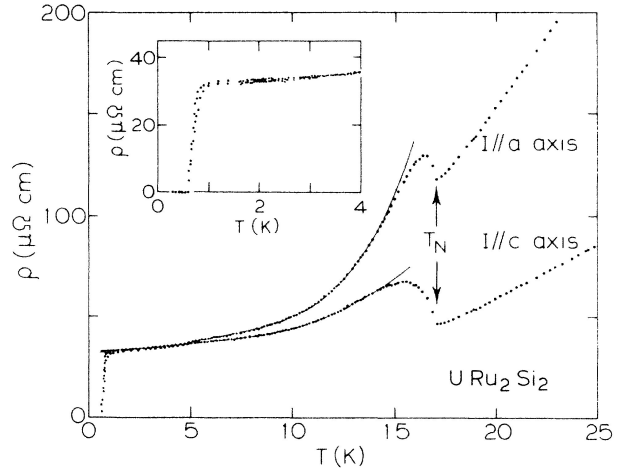


FIG. 3 Susceptibility χ of URu_2Si_2 with applied field (2T) along the a and c axes. Note the deviation from the Curie-Weiss law ($\mu_{\text{eff}} = 3.5 \mu_B/\text{U}$; $\theta_{\text{CW}} = -65 \text{ K}$) along the c -axis below 150 K. After Palstra et al. (1985).



(a) High T



(b) Low T

FIG. 4 Top: Overview of the resistivity ρ along the a and c axes. Bottom: Expanded view of the low-temperature resistivity illustrating the HO transition ($T_o = 17.5 \text{ K}$) and the superconducting one ($T_c = 0.8 \text{ K}$). After Palstra et al. (1986).

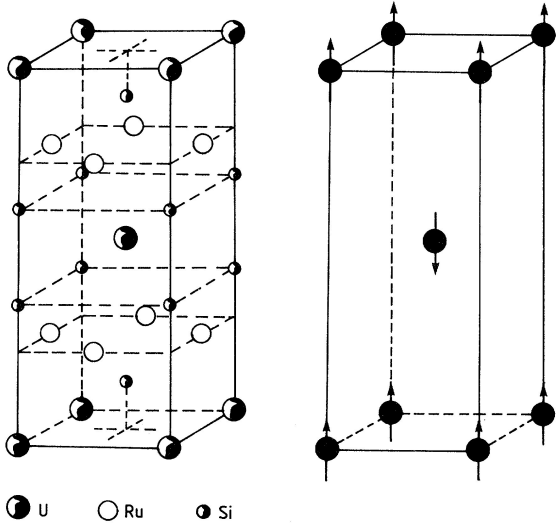


FIG. 5 Left: Crystal structure of body-centered-tetragonal URu_2Si_2 (space group: $I4/mmm$; lattice constants at 4.2 K $a = 4.124 \text{ \AA}$ and $c = 9.582 \text{ \AA}$ after a 0.1 percent contraction from 300 K). Right: the type-I antiferromagnetic c -axis spin alignment of U-moments.

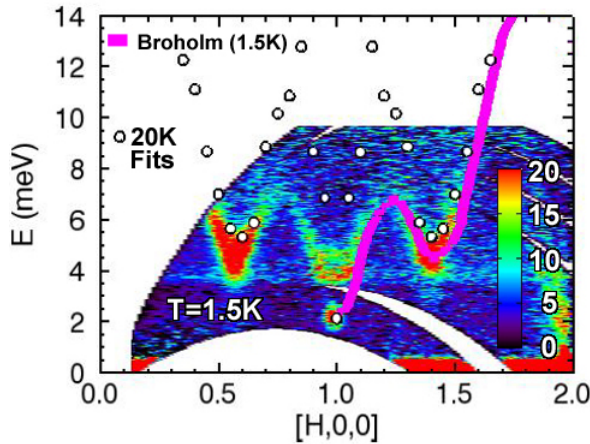


FIG. 6 (Color online) Energy-momentum scan of spin excitations determined by inelastic neutron scattering at 1.5 K (Wiebe et al., 2007). The color bar denotes the intensity of the modes. The two intense modes appear at $\mathbf{Q}_0 = (1, 0, 0)$ and $\mathbf{Q}_1 = (1 \pm 0.4, 0, 0)$ (note that the mode at $(1, 0, 0)$ is partially shaded by the equipment). The purple curve gives the magnon dispersion determined by Broholm et al. (1991). Note also the commensurate gap at $\mathbf{Q}_0 = (1, 0, 0)$ and the larger incommensurate gap at $\mathbf{Q}_1 = (1 \pm 0.4, 0, 0)$. The \mathbf{Q} -independent intensity detected at 3.9 meV is not due to a crystal electrical field excitation, but due to fission processes of ^{235}U . After Janik et al. (2009).

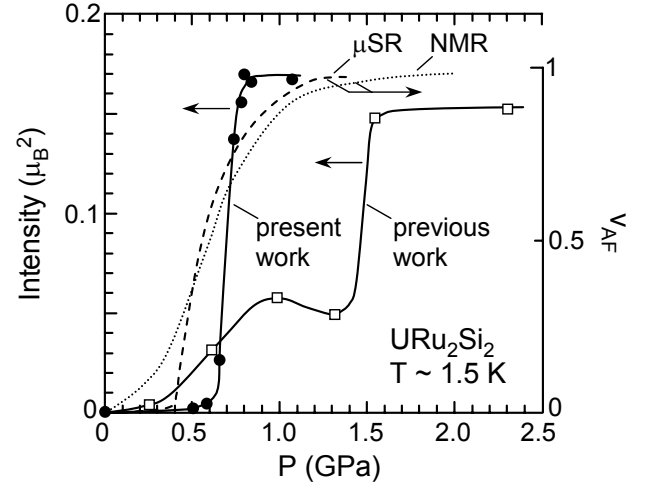


FIG. 7 Influence of the crystal purity on the phase separation between the HO and LMAF phases of URu_2Si_2 . Shown is the pressure dependence of the integrated intensity of the $\mathbf{Q}_0 = (1, 0, 0)$ antiferromagnetic Bragg peak measured at 1.5 K for newer high-purity single crystals (closed circles) and older single crystals (open squares, data from Amitsuka et al. (1999)). Also shown is the pressure dependence of the antiferromagnetic volume fraction (right ordinate) derived from earlier ^{29}Si NMR (Matsuda et al., 2001) and μSR (Amato et al., 2004) measurements. A clear phase transition between the HO and antiferromagnetically ordered phases is present in the purer single crystals. After Amitsuka et al. (2007).

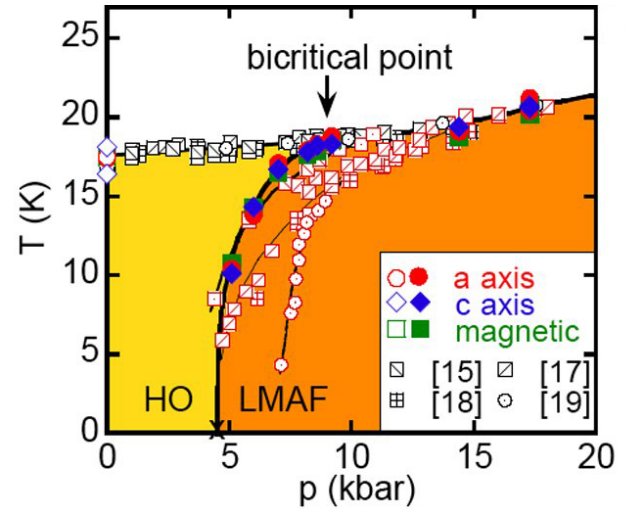


FIG. 8 (Color online) Collection of the up-to-date experimental data representing the temperature-pressure phase diagram of URu_2Si_2 with HO and LMAF ordered states. The upper white region is the heavy Fermi- (or Kondo-) liquid out of which the HO and LMAF develop. [15]: Motoyama et al. (2003), [17]: Hassinger et al. (2008b), [18]: Motoyama et al. (2008), and [19]: Amitsuka et al. (2007). After Niklowitz et al. (2010).

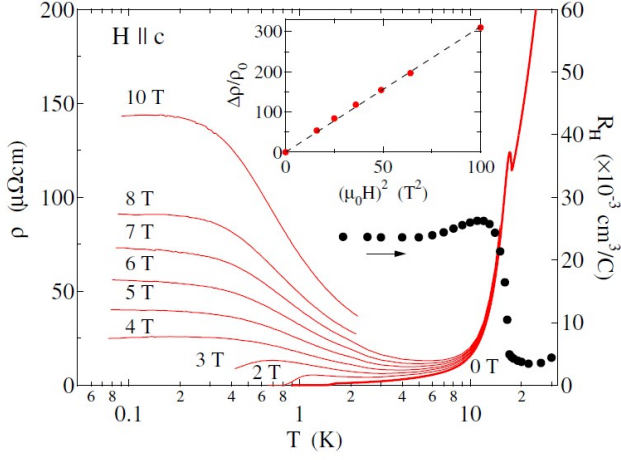


FIG. 9 (Color online) Resistivity as a function of $\log T$ in various magnetic fields (left scale). Hall coefficient through the HO transition (right scale). Inset shows the change of resistivity versus H^2 . From Kasahara et al. (2007).

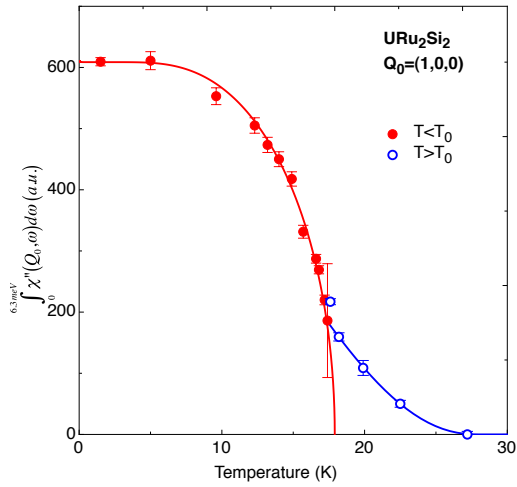
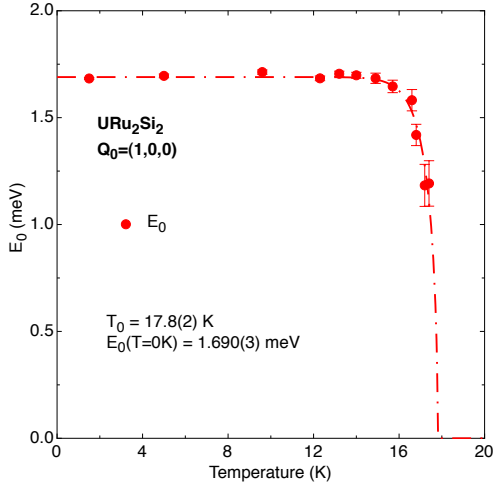


FIG. 10 (Color online) Top: The gapping of the spin resonance at the antiferromagnetic wavevector, $\mathbf{Q}_0 = (1, 0, 0)$ vs. temperature. Note the sudden onset of the spin gap E_0 upon entering the HO state. Bottom: The integrated dynamical spin susceptibility of the antiferromagnetic spin resonance vs. temperature. The integrated intensity displays order parameter behavior and thus tracks the OP of the HO. After Bourdarot et al. (2010).

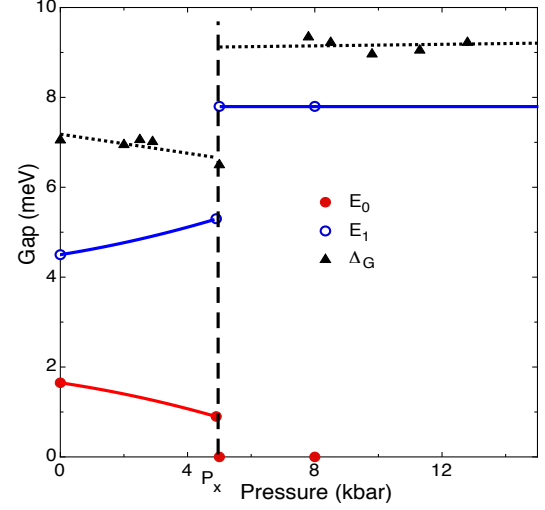


FIG. 11 (Color online) Energy gap scales of HO and LMAF phases determined from INS resonances and bulk resistivity measurements as function of pressure spanning HO to LMAF. Δ_G is the transport gap, whereas E_0 and E_1 are the gaps of the commensurate and incommensurate spin resonances, respectively. After Bourdarot et al. (2010).

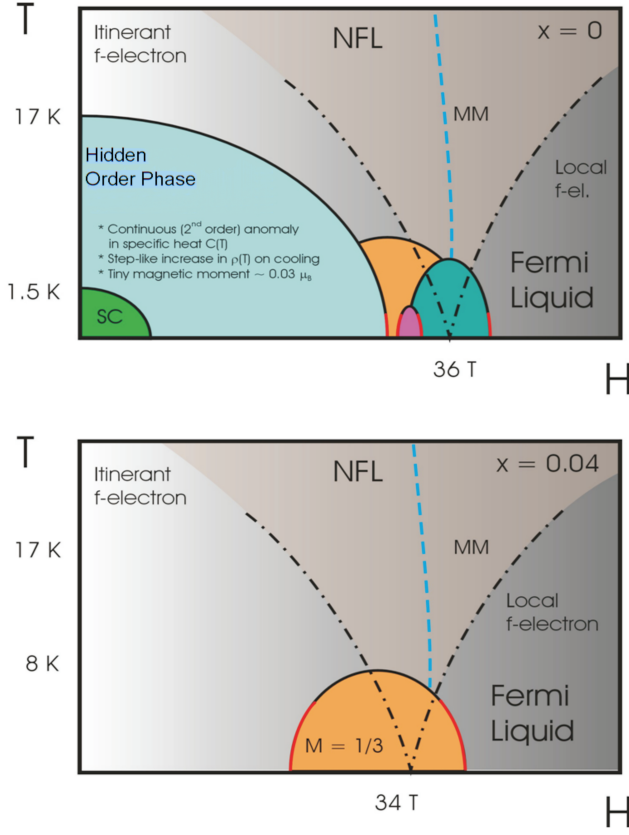


FIG. 12 (Color online) Sketch of the high magnetic field $T - H$ phase diagrams for URu_2Si_2 and $\text{U}(\text{Ru}_{0.96}\text{Rh}_{0.04})_2\text{Si}_2$. MM indicates the metamagnetic transitions, NFL the non-Fermi liquid, and phase II is colored in orange. After Jaime, unpublished (2007).

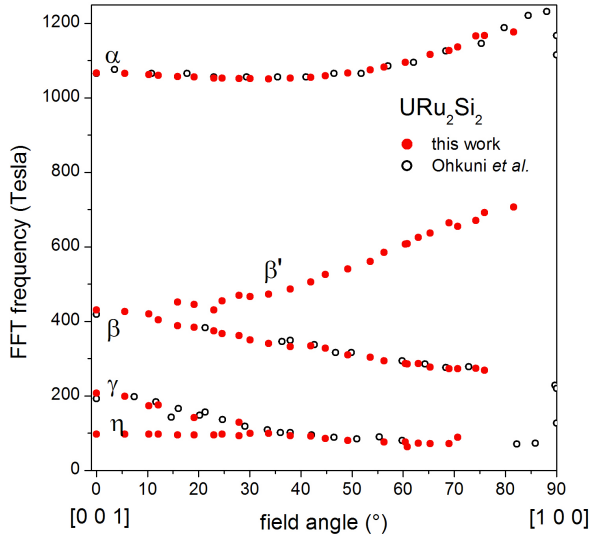


FIG. 13 (Color online) Angular dependence of extremal quantum oscillation frequencies in URu_2Si_2 , comparing the de Haas-van Alphen data of Ohkuni et al. (1999) and the Shubnikov-de Haas data of Hassinger et al. (2010) (labeled ‘this work’). A previously unseen splitting of the β branch was observed, as well as an η orbit that coincides almost with the previously detected γ orbit. Note that the large extremal orbit ε was not detected (cf. Fig. 14). FFT: fast Fourier transform. From Hassinger et al. (2010).

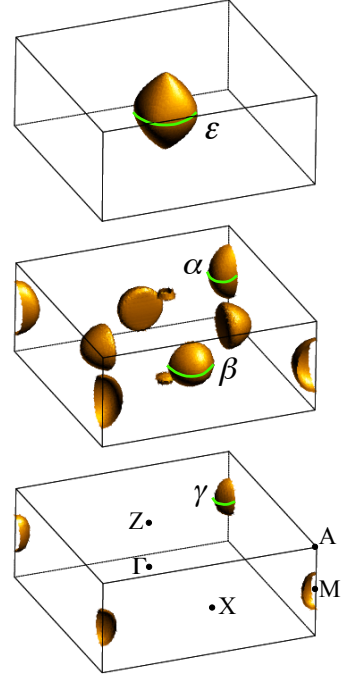


FIG. 14 (Color online) Computed Fermi surface sheets of URu_2Si_2 in the LMAF phase. The extremal Fermi surface orbits for field along the $z = c^*$ axis are indicated by green lines, the branches are labeled by greek letters. Not visible is the small Γ -centered ellipsoid (called η in Fig. 13) that is inside the large Γ -centered surface in the top panel. High-symmetry points are indicated in the bottom panel. After Elgazzar et al. (2009).

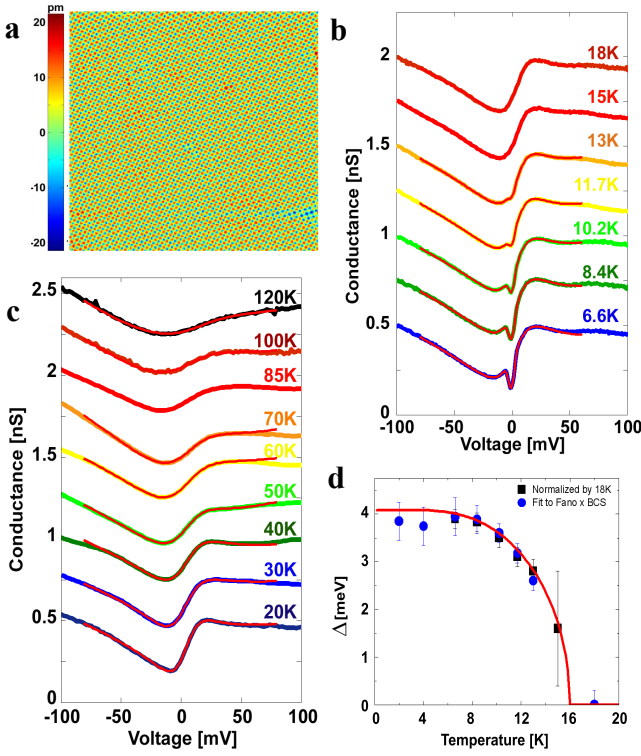


FIG. 15 (Color online) STM and STS spectra of URu_2Si_2 . a) Topological image of the measured U-terminated surface (20 x 20 nm). b) Differential conductance spectrum, dI/dV vs. V , spanning the HO up to T_0 . Note the HO gap appearance within the Fano spectrum. c) Conductance data from 120 to 20 K illustrating the evolution of the Fano resonance. d) Measured temperature dependence of the HO gap Δ . The gap displays an asymmetric BCS-like temperature dependence. Adapted from Aynajian et al. (2010).

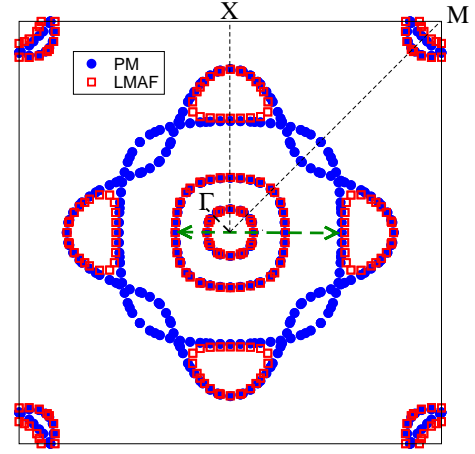


FIG. 16 (Color online) Top: computed energy dispersions of URu_2Si_2 along the Γ -M high-symmetry direction in the ST Brillouin zone. The character of the states responsible for the bands is shown through the colors, where blue color illustrates U 5f character in the paramagnetic (PM) normal state and red color U 5f character in the LMAF phase. Green color depicts the Ru 4d character. The amount of Ru d or U f character is provided through the thickness of the bands. Note that energy dispersions for the PM normal state and LMAF phases are almost on top of each other, but a conspicuous lifting of a band degeneracy and a concomitant opening of a gap occurs between Γ and M. Bottom: cross sections of the PM (blue circles) and the LMAF (red squares) phase in the $k_z = 0$ plane, showing the removal of FS portions in the LMAF phase: the blue FS sections between the rounded half-spheres becomes completely gapped. Other FS are parts are not affected, the LMAF and PM FS cross sections are almost identical. The dashed arrow indicates the nesting vector $0.4 a^*$ (i.e., $(1 \pm 0.4, 0, 0)$ in the BCT structure). Adapted from Oppeneer et al. (2010).

